

Second order asymptotical regularization methods for inverse problems in partial differential equations

YE ZHANG[†]

SCHOOL OF SCIENCE AND TECHNOLOGY, ÖREBRO UNIVERSITY,
70182 ÖREBRO, SWEDEN AND
FACULTY OF MATHEMATICS, CHEMNITZ UNIVERSITY OF TECHNOLOGY,
09107 CHEMNITZ, GERMANY

AND

RONGFANG GONG[‡]

DEPARTMENT OF MATHEMATICS, NANJING UNIVERSITY OF AERONAUTICS AND
ASTRONAUTICS, 211106 NANJING, CHINA

[Received on 23 January 2019]

We develop Second Order Asymptotical Regularization (SOAR) methods for solving inverse source problems in elliptic partial differential equations with both Dirichlet and Neumann boundary data. We show the convergence results of SOAR with the fixed damping parameter, as well as with a dynamic damping parameter, which is a continuous analog of Nesterov's acceleration method. Moreover, by using Morozov's discrepancy principle together with a newly developed total energy discrepancy principle, we prove that the approximate solution of SOAR weakly converges to an exact source function as the measurement noise goes to zero. A damped symplectic scheme, combined with the finite element method, is developed for the numerical implementation of SOAR, which yields a novel iterative regularization scheme for solving inverse source problems. Several numerical examples are given to show the accuracy and the acceleration effect of SOAR. A comparison with the state-of-the-art methods is also provided.

Keywords: Inverse source problems; Partial differential equations; Asymptotical regularization; Convergence; Finite element methods; Symplectic methods.

1. Introduction

In this paper, inspired by the asymptotical regularization (Vainikko & Veretennikov (1986); Tautenhahn (1994); Zhang & Hofmann (2018)), we establish a new framework for stably solving inverse problems in partial differential equations (PDEs). To present the ideas, we take the following inverse source problem as an example: given g_1 and g_2 on Γ , find p such that (p, u) satisfies

$$\begin{cases} -\Delta u + u = p\chi_{\Omega_0} & \text{in } \Omega, \\ u = g_1 \text{ and } \frac{\partial u}{\partial \mathbf{n}} = g_2 & \text{on } \Gamma, \end{cases} \quad (1.1)$$

where $\Omega \subset \mathbb{R}^d$ ($d = 2, 3$) represents a bounded domain with a smooth boundary Γ , $\partial/\partial \mathbf{n}$ stands for the unit outward normal derivative, $\Omega_0 \subset \Omega$ is known as a permissible region of the source function, and χ

[†]Email: ye.zhang@mathematik.tu-chemnitz.de

[‡]Corresponding author. Email: grf_math@nuaa.edu.cn

is the indicator function such that $\chi_{\Omega_0}(x) = 1$ for $x \in \Omega_0$, while $\chi_{\Omega_0}(x) = 0$, when $x \notin \Omega_0$. Note that the framework proposed in this paper can also be applied to various linear and nonlinear inverse problems in PDEs, e.g. inverse source problems in parabolic or hyperbolic PDEs, parameter identification problems in PDEs, etc.

The variational methods of solving (1.1) are usually classified into two groups: the boundary fitting formulation and the domain fitting formulation. For the boundary fitting formulation, we use one of the boundary conditions to form a boundary value problem, and the remaining boundary condition as the object-optimized function to determine the source term. For instance, the following formulation can be considered (Han *et al.* (2006))

$$\min_p \frac{1}{2} \|u(p) - g_1\|_{0,\Gamma}^2, \quad (1.2)$$

where $u(p)$ is the weak solution in $H^1(\Omega)$ of (1.1) with the Neumann boundary condition, and $\|\cdot\|_{0,\Gamma}$ is the standard norm of $L^2(\Gamma)$.

The Kohn-Vogelius method is certainly the most prominent domain fitting formulation for the inverse source problem (1.1). In this approach, the following optimization problem is adopted (Afraites *et al.* (2007); Song & Huang (2012)):

$$\min_p \frac{1}{2} \|u_1(p) - u_2(p)\|_{0,\Omega}^2, \quad (1.3)$$

where $u_1, u_2 \in H^1(\Omega)$ are the weak solutions of $-\Delta u_{1,2} + u_{1,2} = p\chi_{\Omega_0}$ with Dirichlet and Neumann data respectively, and $\|\cdot\|_{0,\Omega}$ is the standard norm of $L^2(\Omega)$.

However, both formulations (1.2) and (1.3) use the Neumann and Dirichlet data separately. In Cheng *et al.* (2014), a novel coupled complex boundary method (CCBM) was introduced. The idea of CCBM is to couple the Neumann data and Dirichlet data in a Robin boundary condition, which leads to the following optimization problem

$$\min_p \frac{1}{2} \|u_{im}\|_{0,\Omega}^2. \quad (1.4)$$

where $u = u_{re} + iu_{im}$ ($i = \sqrt{-1}$ is the imaginary unit) solves

$$\begin{cases} -\Delta u + u = p\chi_{\Omega_0} & \text{in } \Omega, \\ \frac{\partial u}{\partial \mathbf{n}} + iu = g_2 + ig_1 & \text{on } \Gamma. \end{cases} \quad (1.5)$$

Obviously, all formulations (1.2), (1.3) and (1.4) are still ill-posed, since a general source could not be determined uniquely by the boundary measurements, see e.g., Isakov (1990); Alves *et al.* (2009). Moreover, the mapping from the source function to the boundary data is a compact operator in Hilbert spaces, which implies the unboundedness of its inversion operator. Therefore, for the problem with noisy boundary data, regularization methods should be employed for obtaining stable approximate solutions. Loosely speaking, three groups of regularization methods exist: descriptive regularization methods, variational regularization methods and iterative regularization methods.

Descriptive regularization uses a priori information of the solution to overcome the ill-posedness of the original inverse problem. For inverse source problems, under the assumption of sourcewise representation of the unknown source function, the authors in Zhang *et al.* (2018a) combined the expanding compacts method and CCBM to propose a new efficient regularization method. However, in this paper, we are interested in a more general case that no a priori information about the solution is available.

Tikhonov regularization should be the most prominent variational regularization method. Denote $V(p)$ as the objective functional in (1.2), (1.3) or (1.4). With the Tikhonov regularization, the original inverse source problem (1.1) is converted to the following minimization problem:

$$p_\varepsilon = \operatorname{argmin}_p V_\varepsilon(p), \quad V_\varepsilon(p) := V(p) + \frac{\varepsilon}{2} \|p\|_{0,\Omega_0}^2, \quad (1.6)$$

where $\varepsilon > 0$ is a regularization parameter chosen in a special way using the noisy boundary data. Under certain assumptions, (1.6) admits a unique solution p_ε , which converges to the minimal norm solution of (1.1) with the noise-free boundary data (Han *et al.* (2006); Afraites *et al.* (2007); Cheng *et al.* (2014)).

In this paper, our focus is on the iterative regularization approaches, since, from a computational viewpoint, the iterative approach seems more attractable, especially for large-scale problems. The most famous iterative regularization approach should be the Landweber iteration, which is defined by (cf., e.g., Engl *et al.* (1996); Kaltenbacher *et al.* (2008))

$$x_{k+1} = x_k - \Delta t \nabla V(p), \quad (1.7)$$

which can be viewed as a discrete analog of the following first order evolution equation

$$\dot{x}(t) = -\nabla V(p(t)), \quad (1.8)$$

where ∇ denotes the gradient of V , and t is the introduced artificial time. The formulation (1.8) is known as the asymptotical regularization, or the Showalter's method. The regularization property of (1.8) can be analyzed through a proper choice of the terminating time.

It is well known that the original Landweber method works quite slowly. Thus, accelerating strategies are usually adopted in practice. In recent years, there has been increasing evidence to show that the second order iterative methods exhibit remarkable acceleration properties for stably solving ill-posed problems. The most well-known methods are the Nesterov acceleration scheme (Neubauer (2017)), the v -method (Engl *et al.*, 1996, § 6.3), and the two-point gradient method (Hubmer & Ramlau (2017)). Recently, the authors in Zhang & Hofmann (2018) have established an initial theory of the second order asymptotical regularization method with fixed damping parameter for solving general linear ill-posed inverse problems. In this paper, inspired by the development of second order dynamics for accelerating the convergence of iterative regularization methods in Hubmer & Ramlau (2017); Zhang & Hofmann (2018), we develop a second order asymptotical regularization method for solving the inverse source problem (1.1), i.e., we consider the second order evolution equation

$$\begin{cases} \ddot{p}(t) + \eta(t)\dot{p}(t) + \nabla V(p(t)) = 0, \\ p(0) = p_0, \quad \dot{p}(0) = \dot{p}_0, \end{cases} \quad (1.9)$$

where $(p_0, \dot{p}_0) \in P \times P$ is the prescribed initial data, $\eta > 0$ is the so-called damping parameter, which may or may not depend on the artificial time t , and P is the solution space, which will be precisely defined later. It is not difficult to show that the evolution equation (1.9) with the following specific choice of discretization parameters

$$\begin{cases} \Delta t_k = 4 \frac{(2k+2v-1)(k+v-1)}{(k+2v-1)(2k+4v-1)}, \\ \eta_k = \frac{(k+2v-1)(2k+4v-1)(2k+2v-3) - (k-1)(2k-3)(3k+3v-1)}{4(2k+2v-3)(2k+2v-1)(k+v-1)}, \end{cases}$$

yields the v -method. Moreover, as demonstrated in Su *et al.* (2016), (1.9) with a special choice of damping parameter can be considered as an infinite dimensional extension of the Nesterov's scheme in the following sense.

THEOREM 1.1 Let $\{p_k\}$ be the sequence, generated by the Nesterov's scheme with parameters (α, ω) , see (6.4) for details. Then, for all fixed $T > 0$:

$$\lim_{\omega \rightarrow 0} \max_{0 \leq k \leq T/\sqrt{\omega}} \|p_k - p(k\sqrt{\omega})\|_P = 0,$$

where $p(\cdot)$ is the solution of (1.9) with $\eta(t) = \alpha/t$.

The remainder of the paper is structured as follows: Section 2 discusses some properties of the solution of evolution equation (1.9). The convergence analysis for exact and noisy data are presented in Sections 3 and 4, respectively. Finite dimensional approximation of our method is proposed in Section 5, where we develop a novel second order iterative regularization algorithm. Some numerical examples, as well as a comparison with three existing iterative regularization methods, are presented in Section 6. Finally, concluding remarks are given in Section 7.

2. Properties of the second order evolution equation

For clarity, we only consider the formulation (1.4) in this paper. Let us first introduce the notations for the function spaces that are used in this paper. For a set G (e.g., Ω , Ω_0 or Γ), denote by $W^{m,s}(G)$ the Sobolev space with norm $\|\cdot\|_{m,s,G}$. In particular, $L^s(G) := W^{0,s}(G)$. Moreover, $H^m(G)$ represents $W^{m,2}(G)$ with the corresponding inner product $(\cdot, \cdot)_{m,G}$ and norm $\|\cdot\|_{m,G}$. Let $\mathbf{H}^m(G)$ be the complex version of $H^m(G)$ with inner product $((\cdot, \cdot))_{m,G}$ and norm $\|\cdot\|_{m,G}$ defined as follows: $\forall u, v \in \mathbf{H}^m(G)$, $((u, v))_{m,G} = (u, \bar{v})_{m,G}$, $\|u\|_{m,G} = ((u, u))_{m,G}^{1/2}$, where \bar{v} is the conjugate complex of v . Denote $P = L^2(\Omega_0)$ or $H^1(\Omega_0)$ as the space for the source function p . Its corresponding inner product and norm are given by $(\cdot, \cdot)_P$ and $\|\cdot\|_P$, respectively.

Assume that $g_1 \in H^{1/2}(\Gamma) \cap L^\infty(\Gamma)$ and $g_2 \in L^\infty(\Gamma)$. Moreover, instead of the exact data $\{g_1, g_2\}$, we have only the noisy data $g_1^\delta, g_2^\delta \in L^\infty(\Gamma)$ such that

$$\|g_1^\delta - g_1\|_{\infty, \Gamma} \leq \delta, \quad \|g_2^\delta - g_2\|_{\infty, \Gamma} \leq \delta, \quad (2.1)$$

where $\delta > 0$ denotes the error level of the measurement. Then, the CCBM for inverse source problem (1.1) with noisy data $\{g_1^\delta, g_2^\delta\}$ can be formulated as

$$\inf_{p \in P} V(p) = \inf_{p \in P} V(p; \delta) = \inf_{p \in P} \frac{1}{2} \|u_{im}(p)\|_{\delta, \Omega}^2, \quad (2.2)$$

where $u = u_{re} + iu_{im}$ solves

$$\begin{cases} -\Delta u + u = p\chi_{\Omega_0} & \text{in } \Omega, \\ \frac{\partial u}{\partial \mathbf{n}} + iu = g_2^\delta + ig_1^\delta & \text{on } \Gamma. \end{cases} \quad (2.3)$$

Suppose that system (1.1) has at least one solution (p, u) for noise-free data and denote by p^\dagger one of the solutions, i.e.

$$p^\dagger \in \arg \min_{p \in P} V(p; 0). \quad (2.4)$$

PROPOSITION 2.1 (Zhang *et al.*, 2018b, Proposition 1) The Fréchet derivative of $V(p)$, defined in (2.2), is the imaginary part of the solution to the adjoint problem

$$\begin{cases} -\Delta w + w = u_{im}(p) & \text{in } \Omega, \\ \frac{\partial w}{\partial \mathbf{n}} + iw = 0 & \text{on } \Gamma, \end{cases} \quad (2.5)$$

where u_{im} is the imaginary part of u , the solution of (2.3), i.e., $\nabla_p V(p) = w_{im}(p)\chi_{\Omega_0}$.

It is not difficult to show that $V''(p)q^2 = \|u_{im}(q) - u_{im}(0)\|_{0,\Omega}^2$. Hence, $V(p)$ is convex.

Now we are in a position to introduce the second order asymptotical regularization for solving the inverse source problem (1.1).

DEFINITION 2.2 An element $p^\delta(x, T^*) \in P$ with an appropriate selected terminating time point $T^* = T^*(\delta)$ is called a second order asymptotical regularized solution if $p^\delta(x, t)$ is the solution to the following Cauchy problem

$$\begin{cases} \ddot{p}^\delta(x, t) + \eta(t)\dot{p}^\delta(x, t) + w_{im}(x, t) = 0, & x \in \Omega_0, t \in (0, \infty), \\ p^\delta(x, 0) = p_0(x), \dot{p}^\delta(x, 0) = \dot{p}_0(x), & x \in \Omega_0, \end{cases} \quad (2.6)$$

where $w = w_{re} + iw_{im}$ is the solution of the adjoint problem with the same t

$$\begin{cases} -\Delta w(x, t) + w(x, t) = u_{im}(p^\delta(x, t)), & x \in \Omega, t \in (0, \infty), \\ \frac{\partial w(x, t)}{\partial \mathbf{n}} + iw(x, t) = 0, & x \in \Gamma, t \in (0, \infty), \end{cases} \quad (2.7)$$

and $u = u_{re} + iu_{im}$ is the solution of the BVP

$$\begin{cases} -\Delta u(x, t) + u(x, t) = p^\delta(x, t)\chi_{\Omega_0}, & x \in \Omega, t \in (0, \infty), \\ \frac{\partial u(x, t)}{\partial \mathbf{n}} + iu(x, t) = g_2^\delta(x) + ig_1^\delta(x), & x \in \Gamma, t \in (0, \infty). \end{cases} \quad (2.8)$$

Before presenting the solvability of system (2.6)-(2.8), we discuss the well-posedness of the BVPs (2.7) and (2.8). For any $u, \psi \in \mathbf{H}^1(\Omega)$, define

$$\begin{aligned} a(u, \psi) &= \int_{\Omega} (\nabla u \cdot \nabla \bar{\psi} + u \bar{\psi}) dx + i \int_{\Gamma} u \bar{\psi} ds, \\ f^\delta(\psi) &= \int_{\Omega_0} p^\delta \bar{\psi} dx + \int_{\Gamma} g_2^\delta \bar{\psi} ds + i \int_{\Gamma} g_1^\delta \bar{\psi} ds. \end{aligned}$$

Then the weak form of the BVP (2.8) reads:

$$\text{find } u \in \mathbf{H}^1(\Omega) \text{ such that } a(u, \psi) = f^\delta(\psi), \quad \forall \psi \in \mathbf{H}^1(\Omega). \quad (2.9)$$

LEMMA 2.1 (Cheng *et al.* (2014)) Problem (2.9) admits a unique solution $u \in \mathbf{H}^1(\Omega)$ which depends continuously on p^δ, g_1^δ and g_2^δ . Furthermore, a constant $C(\Omega)$ exists such that

$$\|u\|_{1,\Omega} \leq C(\Omega) \left(\|p^\delta\|_{0,\Omega_0} + \|g_1^\delta\|_{0,\Gamma} + \|g_2^\delta\|_{0,\Gamma} \right). \quad (2.10)$$

By Lemma 2.1 and the definition of $V(p)$ in (2.2) and w in (2.5), it is not difficult to prove the following lemma.

LEMMA 2.2 The following two inequalities hold for some constants $C(\Omega)$:

$$V(p^\delta) \leq C(\Omega) \left(\|p^\delta\|_{0,\Omega_0}^2 + \|g_1^\delta\|_{0,\Gamma}^2 + \|g_2^\delta\|_{0,\Gamma}^2 \right), \quad (2.11)$$

$$\|w(p^\delta)\|_{1,\Omega} \leq C(\Omega) \left(\|p^\delta\|_{0,\Omega_0} + \|g_1^\delta\|_{0,\Gamma} + \|g_2^\delta\|_{0,\Gamma} \right). \quad (2.12)$$

THEOREM 2.3 For each pair $(p_0, \dot{p}_0) \in P \times P$, system (2.6)-(2.8) has a unique weak solution which depends continuously on the boundary data $\{g_1^\delta, g_2^\delta\}$.

The proof is similar to those of (a) in (Zhang *et al.*, 2018b, Theorem 1). A sketch of the proof is given in the Appendix A.

3. Convergence for noise-free boundary data

In this section, we investigate two models: when the damping parameter η is fixed, and when it is time dependent. For simplicity, sometimes let $p(t) = p(\cdot, t)$.

3.1 Case I: η is a constant

We first study the dynamics of the solution $p(t) \in P$ of system (2.6)-(2.8).

LEMMA 3.1 Let $p(x, t)$ be the solution of (2.6)-(2.8) with the exact data $\{g_1, g_2\}$. Then, in the case $\eta \geq 1$, we have

- (i) $p \in L^\infty([0, \infty), P)$.
- (ii) $\dot{p} \in L^\infty([0, \infty), P) \cap L^2([0, \infty), P)$ and $\dot{p}(\cdot, t) \rightarrow 0$ as $t \rightarrow \infty$.
- (iii) $\ddot{p} \in L^\infty([0, \infty), P) \cap L^2([0, \infty), P)$ and $\ddot{p}(\cdot, t) \rightarrow 0$ as $t \rightarrow \infty$.
- (iv) $V(p(\cdot, t)) = o(t^{-1})$ as $t \rightarrow \infty$.

Proof. The proof follows the idea in Attouch *et al.* (2000). Consider for every $t \in [0, \infty)$ the function $e(t) = e(t; p^\dagger) = \frac{1}{2} \|p(t) - p^\dagger\|_P^2$, where p^\dagger is defined in (2.4). Since $\dot{e}(t) = (p(t) - p^\dagger, \dot{p}(t))_P$ and $\ddot{e}(t) = \|\dot{p}(t)\|_P^2 + (p(t) - p^\dagger, \ddot{p}(t))_P$ for every $t \in [0, \infty)$, taking into account (1.9), we get

$$\ddot{e}(t) + \eta \dot{e}(t) + (p(t) - p^\dagger, u_{im}(p(t)))_P = \|\dot{p}(t)\|_P^2. \quad (3.1)$$

Here, and later on, we denote $(p, u)_P = \int_{\Omega_0} p u dx$ for $P = L^2(\Omega_0)$ and $(p, u)_P = \int_{\Omega_0} p u dx + \int_{\Omega_0} \frac{\partial p}{\partial x} \frac{\partial u}{\partial x} dx$ for $P = H^1(\Omega_0)$. Moreover, $\|u\|_P = \sqrt{(u, u)_P}$.

On the other hand, by the convexity inequality of the functional $\|u_{im}(\cdot)\|_P^2$, we derive

$$\|u_{im}(p(t))\|_P^2 = \|u_{im}(p(t))\|_P^2 - \|u_{im}(p^\dagger)\|_P^2 \leq (p(t) - p^\dagger, u_{im}(p(t)))_P. \quad (3.2)$$

Combine (3.1) and the above inequality to obtain

$$\ddot{e}(t) + \eta \dot{e}(t) + \|u_{im}(p(t))\|_P^2 \leq \|\dot{p}(t)\|_P^2 \quad (3.3)$$

or, equivalently (by using the equation (2.6)),

$$\ddot{e}(t) + \eta \dot{e}(t) + \eta \frac{d\|\dot{p}(t)\|_P^2}{dt} + (\eta^2 - 1) \|\dot{p}(t)\|_P^2 + \|\ddot{p}\|_P^2 \leq 0. \quad (3.4)$$

By the assumption $\eta \geq 1$, we deduce that

$$\ddot{e}(t) + \eta \dot{e}(t) + \eta \frac{d\|\dot{p}(t)\|_P^2}{dt} \leq 0, \quad (3.5)$$

which means that the function $t \mapsto \dot{e}(t) + \eta e(t) + \eta \|\dot{p}(t)\|_P^2$ is monotonically decreasing. Hence a real number C exists such that

$$\dot{e}(t) + \eta e(t) + \eta \|\dot{p}(t)\|_P^2 \leq C, \quad (3.6)$$

which implies $\dot{e}(s) + \eta e(s) \leq C$. By multiplying this inequality with $e^{\eta s}$ and then integrating from 0 to t , we obtain the inequality

$$e(t) \leq e(0)e^{-\eta t} + C(1 - e^{-\eta t})/\eta \leq e(0) + C/\eta.$$

Hence, $e(\cdot)$ is uniform bounded, and, consequently, $p(\cdot) \in L^\infty([0, \infty), P)$.

Now, consider the long-term behavior of \dot{p} . Define the Lyapunov function of the differential equation (2.6) by $\mathcal{E}(t) = V(p(t)) + \frac{1}{2}\|\dot{p}(t)\|_P^2$. It is not difficult to show that

$$\dot{\mathcal{E}}(t) = -\eta\|\dot{p}(t)\|_P^2 \quad (3.7)$$

by looking at the equation (2.6) and the differentiation of the energy function $\dot{\mathcal{E}}(t) = (\dot{p}(t), \dot{p}(t) - u_{im}(p(t)))_P$. Hence, $\mathcal{E}(t)$ is non-increasing, and consequently, $\|\dot{p}(t)\|_P^2 \leq 2\mathcal{E}(0)$. Therefore, $\dot{p}(\cdot) \in L^\infty([0, \infty), P)$. Integrating both sides in (3.7), we obtain

$$\int_0^\infty \|\dot{p}(t)\|_P^2 dt \leq \mathcal{E}(0)/\eta < \infty,$$

which yields $\dot{p}(\cdot) \in L^2([0, \infty), P)$ (and $\lim_{t \rightarrow \infty} \dot{p}(t) = 0$ since $\dot{p}(\cdot) \in L^\infty([0, \infty), P) \cap L^2([0, \infty), P)$).

Define

$$h(t) = \frac{\eta}{2}\|p(t) - p^\dagger\|_P^2 + (\dot{p}(t), p(t) - p^\dagger)_P. \quad (3.8)$$

By elementary calculations, we derive that

$$\begin{aligned} \dot{h}(t) &= \eta(\dot{p}(t), p(t) - p^\dagger)_P + (\ddot{p}(t), p(t) - p^\dagger)_P + \|\dot{p}(t)\|_P^2 \\ &= \|\dot{p}(t)\|_P^2 - (u_{im}(p(t)), p(t) - p^\dagger)_P, \end{aligned}$$

which implies that (by noting $\dot{\mathcal{E}}(t) = -\eta\|\dot{p}(t)\|_P^2$ and the inequality (3.2))

$$3\dot{\mathcal{E}}(t) + 2\eta\mathcal{E}(t) + \eta\dot{h}(t) = \eta [2V(p(t)) - (p - p^\dagger, u_{im}(p(t)))_P] \leq 0.$$

Integrate the above inequality on $[0, T]$ to obtain together with the non-negativity of $\mathcal{E}(t)$

$$\int_0^T \mathcal{E}(t) dt \leq \frac{3}{2\eta} (\mathcal{E}(0) - \mathcal{E}(T)) - \frac{1}{2}(h(T) - h(0)) \leq \left(\frac{3}{2\eta} \mathcal{E}(0) + \frac{1}{2}h(0) \right) - \frac{1}{2}h(T). \quad (3.9)$$

On the other hand, since both $p(t)$ and $\dot{p}(t)$ are uniform bounded, a constant M exists such that $|h(t)| \leq M$. Hence, letting $T \rightarrow \infty$ in (3.9), we obtain

$$\int_0^\infty \mathcal{E}(t) dt < \infty. \quad (3.10)$$

Hence $\lim_{t \rightarrow \infty} \mathcal{E}(t) = 0$, and, consequently, $\lim_{t \rightarrow \infty} \dot{p}(t) = 0$.

Since $\mathcal{E}(t)$ is non-increasing, we deduce that

$$\int_{T/2}^T \mathcal{E}(t) dt \geq \frac{T}{2} \mathcal{E}(T). \quad (3.11)$$

Using (3.10), the left side of (3.11) tends to 0 when $T \rightarrow \infty$, which implies that $\lim_{T \rightarrow \infty} T\mathcal{E}(T) = 0$. Hence, we conclude $\lim_{T \rightarrow \infty} TV(p(T)) = 0$, which yields the desired result in (iv).

Finally, let us show the long-term behavior of $\ddot{p}(t)$. Integrating the inequality (3.4) from 0 to T we obtain that there exists a real number C' such that for every $t \in [0, \infty)$

$$\dot{e}(T) + \eta e(T) + \eta\|\dot{p}(T)\|_P^2 + (\eta^2 - 1) \int_0^T \|\dot{p}(t)\|_P^2 dt + \eta \int_0^T \|\ddot{p}(t)\|_P^2 dt \leq C'. \quad (3.12)$$

Since both $e(\cdot)$ and $\dot{e}(\cdot)$ are global bounded (note that $p(t), \dot{p}(t) \in L^\infty([0, \infty), P)$), inequality (3.12) gives $\ddot{p}(t) \in L^2([0, \infty), P)$. The relations $\ddot{p}(t) \in L^\infty([0, \infty), P)$ and $\ddot{p}(t) \rightarrow 0$ as $t \rightarrow \infty$ are obvious by noting assertions (i), (ii), (iv) and the connection equation (1.9). \square

REMARK 3.1 The rate $V(p(\cdot, t)) = o(t^{-1})$ as $t \rightarrow \infty$ given in Lemma 3.1 for the second order evolution equation (1.9) should be compared with the corresponding result for the first order method, i.e. the gradient decent methods, where one only obtains $V(p(\cdot, t)) = \mathcal{O}(t^{-1})$ as $t \rightarrow \infty$. If we consider a discrete iterative method with the number k of iterations, assertion (iv) in Lemma 3.1 indicates that in comparison with gradient descent methods, the second order methods (1.9) need the same computational complexity for the number k of iterations, but can achieve a higher order $o(k^{-1})$ of accuracy of the objective functional.

Now, we list the following two lemmas, which will be used in the convergence analysis of the dynamical solution $p(x, t)$.

LEMMA 3.2 (Opial lemma Opial (1967)) Let P be a Hilbert space and $p : [0, \infty) \rightarrow P$ be a mapping such that there exists a non-empty set $S \subset P$ which satisfies

- (i) $\forall t_n \rightarrow \infty$ with $p(t_n) \rightharpoonup \bar{p}$ weakly in P , we have $\bar{p} \in S$.
- (ii) $\forall p^\dagger \in S$, $\lim_{t \rightarrow \infty} \|p(t) - p^\dagger\|_P$ exists.

Then, $p(t)$ weakly converges as $t \rightarrow \infty$ to some element of S .

LEMMA 3.3 (Lemma 4.2 in Attouch *et al.* (2000)) Let $\varphi(t) \in C^1((0, \infty), [0, +\infty))$ satisfy the inequality $\ddot{\varphi}(t) + \eta\dot{\varphi}(t) \leq g(t)$ with $g(t) \in L^1((0, \infty), [0, +\infty))$. Then, $\dot{\varphi}_+$, the positive part of $\dot{\varphi}$, belongs to $L^1((0, \infty), [0, +\infty))$ and, as a consequence, $\lim_{t \rightarrow \infty} \varphi(t)$ exists.

Now, we are in the position to present the main result in this section.

THEOREM 3.1 The solution $p(x, t)$ of (2.6)-(2.8) with the exact data converges weakly in P to an exact source function of inverse source problem (1.1) as $t \rightarrow \infty$.

Proof. It suffices to check two conditions in Opial lemma. Consider a sequence $\{p(t_n)\}$ such that $p(t_n) \rightharpoonup \bar{p}$ weakly in P . Applying the convexity inequality to the functional $V(p) = \frac{1}{2}\|u_{im}\|_{0, \Omega}^2$ we have

$$V(z) \geq V(p(t_n)) + (z - p(t_n), \nabla V(p(t_n)))_P, \quad \forall z \in P. \quad (3.13)$$

By using the continuity of $V(p)$, and noticing that, in the inner product $(z - p(t_n), \nabla V(p(t_n)))_P$, the two terms are, respectively, norm converging to zero and weakly convergent, we can pass to the lower limit to obtain $V(z) \geq V(p(t_n))$ for all $z \in P$. Set $z = p^\dagger$ in the above inequality, we conclude that $0 = V(p^\dagger) \geq V(\bar{p})$, which implies that \bar{p} is also a solution of inverse source problem (1.1).

Now, we prove the second requirement in Lemma 3.2. It is equivalent to show that $\lim_{t \rightarrow \infty} e(t)$ exists, where $e(t) = \frac{1}{2}\|p(t) - p^\dagger\|_P^2$ is defined in the proof of Lemma 3.1. From (3.3), we deduce that

$$\ddot{e}(t) + \eta\dot{e}(t) \leq \|\dot{p}(t)\|_P^2. \quad (3.14)$$

Since $\dot{p}(\cdot) \in L^2([0, \infty), P)$, inequality (3.14) together with Lemma (3.3) yields the second condition in Opial lemma. This completes the proof of the weak convergence of the dynamical solution of (1.9). \square

3.2 Case II: $\eta(t) = r/t$

Now, we study the second order dynamical system (2.6)-(2.8) with an asymptotical vanishing damping parameter of the type $\eta(t) = r/t$, i.e. we consider the following evolution equation

$$\begin{cases} \ddot{p}(x, t) + \frac{r}{t}\dot{p}(x, t) + w_{im}(x, t) = 0, & x \in \Omega_0, t \in (1, \infty), \\ p(x, 1) = p_0(x), \dot{p}(x, 1) = \dot{p}_0(x), & x \in \Omega_0, \end{cases} \quad (3.15)$$

where $w = w_{re} + iw_{im}$ is the solution of the adjoint problem (2.7) with the same t . As discussed in Section 1, this is a particularly interesting case as the second order flow (3.15) yields a continuous version of Nesterov's scheme, which has a higher order of convergence rate for the residual functional, i.e. $V(p(\cdot, t)) = \mathcal{O}(k^{-2})$ for $r = 3$ and $V(p(\cdot, t)) = o(k^{-2})$ for $r > 3$ (Attouch & Peypouquet (2016)).

REMARK 3.2 We shift the initial time point from 0 to 1 for the regularity of the term r/t . Otherwise, one can use $r/(t+1)$ instead of r/t in (3.15).

For proving the following assertions, we introduce the anchored energy function

$$\mathcal{E}_\lambda(t) = t^2 V(p(t)) + \frac{1}{2} \|\lambda(p(t) - p^\dagger) + t\dot{p}(t)\|_P^2 + \frac{\lambda(r-1-\lambda)}{2} \|p(t) - p^\dagger\|_P^2, \quad (3.16)$$

where the exact source p^\dagger is given in (2.4). For $r \geq 3$, using the convexity inequality $0 = V(p^\dagger) \geq V(p) + \langle \nabla V(p), p^\dagger - p \rangle_P$ for all $p \in P$ and (3.15), it is not difficult to show that

$$\dot{\mathcal{E}}_\lambda(t) \leq -(\lambda - 2)tV(p(t)) - (r-1-\lambda)t\|\dot{p}(t)\|_P^2. \quad (3.17)$$

Hence, for $r \geq 3$ and $\lambda \in [2, r-1]$, $\mathcal{E}_\lambda(t)$ is non-increasing.

Now, we are in position to derive similar results to those in Section 3.1.

LEMMA 3.4 Let $p(x, t)$ be the solution of (3.15) with the exact data. Then, $\dot{p} \in L^\infty([1, \infty), P) \cap L^2([1, \infty), P)$ and $\dot{p}(\cdot, t) \rightarrow 0$ as $t \rightarrow \infty$. Moreover, $V(p(\cdot, t)) = \mathcal{O}(t^{-2})$ as $t \rightarrow \infty$.

Proof. This proof uses the technique in Attouch *et al.* (2018). Consider the Lyapunov function of (3.15) by $\mathcal{E}(t) = \frac{1}{2} \|\dot{p}(t)\|_P^2 + V(p(t))$. It is easy to show that

$$\dot{\mathcal{E}}(t) = -\frac{r}{t} \|\dot{p}(t)\|_P^2 \leq 0. \quad (3.18)$$

Hence, $\mathcal{E}(t)$ is non-increasing, and $\mathcal{E}(\infty) := \lim_{t \rightarrow \infty} \mathcal{E}(t)$ exists by noting that $\mathcal{E}(t) \geq 0$ for all t . Furthermore, by $\|\dot{p}(t)\|_P^2 \leq 2\mathcal{E}(t) \leq 2\mathcal{E}(1)$ we conclude the uniform boundedness of $\dot{p}(\cdot)$.

Integrating both sides in (3.18), we obtain

$$\int_1^\infty \|\dot{p}(t)\|_P^2 dt \leq \int_1^\infty t \|\dot{p}(t)\|_P^2 dt \leq \mathcal{E}(1)/r < \infty,$$

which yields $\dot{p}(\cdot) \in L^2([1, \infty), P)$. Now, consider the function $e(t) = \frac{1}{2} \|p(t) - p^\dagger\|_P^2$. Using the local convexity of $V(\cdot)$ and the equation (1.9), similar to (3.3), it is not difficult to obtain

$$\ddot{e}(t) + \frac{r}{t} \dot{e}(t) + V(p(t)) \leq \|\dot{p}(t)\|_P^2. \quad (3.19)$$

Divide this expression by t to obtain

$$\frac{1}{t} \ddot{e}(t) + \frac{r}{t^2} \dot{e}(t) + \frac{1}{t} \mathcal{E}(t) \leq \frac{3}{2t} \|\dot{p}(t)\|_P^2,$$

Integrating above inequality from 1 to t and using integration by parts for $\ddot{e}(t)$, we obtain

$$\int_1^t \frac{\mathcal{E}(\tau)}{\tau} d\tau \leq \dot{e}(1) - \frac{\dot{e}(t)}{t} - (r+1) \int_1^t \frac{\dot{e}(\tau)}{\tau^2} d\tau + \frac{3}{2} \int_1^t \frac{\|\dot{p}(\tau)\|_P^2}{\tau} d\tau. \quad (3.20)$$

On one hand, using the integration by parts and the positivity of functional $e(\cdot)$, we have

$$\int_1^t \frac{\dot{e}(\tau)}{\tau^2} d\tau = \frac{e(t)}{t^2} - e(1) + 2 \int_1^t \frac{e(\tau)}{\tau^3} d\tau \geq -e(1). \quad (3.21)$$

On the other hand, relation (3.18) gives

$$\int_1^t \frac{\|\dot{p}(\tau)\|_P^2}{\tau} d\tau = \frac{\mathcal{E}(1) - \mathcal{E}(t)}{r}. \quad (3.22)$$

Combine (3.20)-(3.22) to get

$$\int_1^t \frac{\mathcal{E}(\tau)}{\tau} d\tau \leq \dot{e}(1) - \frac{\dot{e}(t)}{t} + (r+1)e(1) + \frac{3(\mathcal{E}(1) - \mathcal{E}(t))}{2r} = C(1) - \frac{\dot{e}(t)}{t} - \frac{3\mathcal{E}(t)}{2r}, \quad (3.23)$$

where $C(1) = \dot{e}(1) + (r+1)e(1) + \frac{3\mathcal{E}(1)}{2r}$ collects the constant terms. For any $T \geq t > 1$, we have

$$\mathcal{E}(T) \int_1^t \frac{1}{\tau} d\tau + \frac{3\mathcal{E}(T)}{2r} \leq C(1) - \frac{\dot{e}(t)}{t} \quad (3.24)$$

by noting the non-increasing of Lyapunov function $\mathcal{E}(t)$. Rewrite (3.24) as $\mathcal{E}(T) (\ln(t) + \frac{3}{2r}) \leq C(1) - \frac{\dot{e}(t)}{t}$, and then integrate it from $t = 1$ to $t = T$ to have

$$\mathcal{E}(T) \left(T \ln(T) + 1 - T + \frac{3}{2r}(T-1) \right) \leq C(1)(T-1) - \int_1^T \frac{\dot{e}(t)}{t} dt. \quad (3.25)$$

Moreover, using the integration by parts and the positivity of functional $e(\cdot)$, we have

$$\int_1^T \frac{\dot{e}(t)}{t} dt = \frac{e(T)}{T} - e(1) + \int_1^T \frac{e(t)}{t^2} dt \geq -e(1). \quad (3.26)$$

By combining (3.25) and (3.26), we deduce that

$$\mathcal{E}(T) (T \ln(T) + C_1 T + C_2) \leq C(1)T + C_3, \quad (3.27)$$

where $C_1 = \frac{3}{2r} - 1$, $C_2 = 1 - 3/(2r)$ and $C_3 = e(1) - C(1)$ are three constants.

Inequality (3.27) immediately yields $\mathcal{E}(\infty) \leq 0$. By the non-negativity of Lyapunov function $\mathcal{E}(\cdot)$, we conclude $\mathcal{E}(\infty) = 0$, which implies that both $\dot{p}(T)$ and $V(p(T))$ converge to 0 in P when $T \rightarrow \infty$.

Finally, let us show the convergence rate of $V(p(t))$. Set $\lambda = r - 1$ in (3.16) to obtain $t^2 V(p(t)) \leq \mathcal{E}_{r-1}(t)$. Since $\mathcal{E}_{r-1}(t)$ is non-increasing, we conclude that $V(p(t)) \leq \mathcal{E}_{r-1}(1)/t^2$. \square

LEMMA 3.5 (Lemma 5.9 in Attouch *et al.* (2018)) Let $\varphi(t) \in C^1((1, \infty), [0, +\infty))$ satisfy the inequality $t\dot{\varphi}(t) + r\varphi(t) \leq g(t)$ with $r \geq 1$ and $g(t) \in L^1((1, \infty), [0, +\infty))$. Then, φ_+ , the positive part of φ , belongs to $L^1((1, \infty), [0, +\infty))$ and, as a consequence, $\lim_{t \rightarrow \infty} \varphi(t)$ exists.

THEOREM 3.2 The solution $p(x, t)$ of (3.15) with $r > 3$ converges weakly to an exact source function of inverse source problem (1.1) as $t \rightarrow \infty$.

Proof. Set $\lambda = 2$ in (3.16) to derive $\|p(t) - p^\dagger\|_P^2 \leq \frac{\mathcal{E}_2(t)}{r-3} \leq \frac{\mathcal{E}_2(1)}{r-3}$, which yields the uniform boundedness of $p(t)$. Furthermore, we have

$$\dot{\mathcal{E}}_2(t) \leq -(r-3)t\|\dot{p}(t)\|_P^2. \quad (3.28)$$

Integrating (3.28) from 1 to T , and recalling that $\mathcal{E}_2(t)$ is non-negative, we obtain

$$\int_1^T t\|\dot{p}(t)\|_P^2 dt \leq \mathcal{E}_2(1)/(r-3). \quad (3.29)$$

Let $T \rightarrow \infty$ to conclude $t\|\dot{p}(t)\|_P^2 \in L^1((1, \infty), [0, \infty))$. Recall from (3.19) to obtain $t\ddot{e}(t) + r\dot{e}(t) \leq t\|\dot{p}(t)\|_P^2$. From Lemma 3.5, and note that $t\|\dot{p}(t)\|_P^2$ is integrable on $[1, \infty)$, the limit $\lim_{t \rightarrow \infty} e(t)$ exists. This gives the second hypothesis in Opial's Lemma. The first one was established in Lemma 3.4, i.e. $V(p(t)) \rightarrow 0$ as $t \rightarrow \infty$. This completes the proof by using the Opial's Lemma 3.2. \square

REMARK 3.3 (a) In Theorems 3.1 and 3.2, we only obtain the weak convergence for both fixed and dynamic damping parameters. One way to obtain the strong convergence result is to include a regularization term $\varepsilon(t)p(x, t)$ in the evolution equation (1.9) with a specially chosen dynamic regularization parameter $\varepsilon(t)$, see Zhang *et al.* (2018b) for details. However, the numerical results in Section 6 show that our method works much better than this method in terms of accuracy and speed.

(b) Let Π^h be any project operator, acting from P into a finite element space P^h for a fixed triangulation \mathcal{T}^h . Then, we have the strong convergence $\Pi^h p^\delta(\cdot, t) \rightarrow \Pi^h p^\dagger(\cdot)$ as $t \rightarrow \infty$ in P^h , since strong convergence and weak convergence coincide in any finite dimensional/element space. This fact will be used in Theorem 5.4 about the strong convergence of the finite element solution.

4. Convergence for noisy data

In this section, we investigate the regularization property of the dynamic solution $p^\delta(\cdot, t)$ of (2.6)-(2.8), equipped with some appropriate selection rules of the terminating time T^* .

PROPOSITION 4.1 There exists a constant $C_0(\Omega)$, depending only on the geometry of the domain Ω , such that $\|u_{im}(p^\dagger)\|_{0, \Omega} \leq C_0(\Omega)\delta$, where $u = u_{re} + iu_{im}$ solves (2.3) and p^\dagger is defined in (2.4). Consequently, we have $V(p^\dagger) \leq C_0^2\delta^2$. If Ω is a ball in \mathbb{R}^d centered at 0 with radius R or an annulus in \mathbb{R}^d centered at 0 with radius R and $r(< R)$, we have

$$C_0(\Omega) = \max(d, R)(2\pi)^{1/2}. \quad (4.1)$$

Proof. Denote by \tilde{u} the weak solution of (2.3) with the exact source term p^\dagger . Define $v := u - \tilde{u}$. Then v satisfies

$$\begin{cases} -\Delta v + v = 0 & \text{in } \Omega, \\ \frac{\partial v}{\partial \mathbf{n}} + iv = (g_2^\delta - g_2) + i(g_1^\delta - g_1) & \text{on } \Gamma. \end{cases} \quad (4.2)$$

The weak form of the above BVP (4.2) reads:

$$\text{find } v \in \mathbf{H}^1(\Omega) \text{ such that } a(v, \psi) = \tilde{f}^\delta(\psi), \quad \forall \psi \in \mathbf{H}^1(\Omega), \quad (4.3)$$

where $\tilde{f}^\delta(\psi) = \int_\Gamma (g_2^\delta - g_2)\bar{\psi} ds + i \int_\Gamma (g_1^\delta - g_1)\bar{\psi} ds$. Denote by v_{re} and v_{im} the real and imaginary parts of v , respectively. Obviously, $v_{im} \equiv u_{im}$ by noting $\tilde{u}_{im} = 0$. Furthermore, if one separates the real and imaginary parts of problem (4.2), the real part v_{re} of v satisfies

$$\begin{cases} -\Delta v_{re} + v_{re} = 0 & \text{in } \Omega, \\ \frac{\partial v_{re}}{\partial \mathbf{n}} - v_{im} = g_2^\delta - g_2 & \text{on } \Gamma, \end{cases}$$

whose weak form is

$$\int_{\Omega} (\nabla v_{re} \cdot \nabla \psi + v_{re} \psi) dx = \int_{\Gamma} (g_2^{\delta} - g_2) \psi ds + \int_{\Gamma} v_{im} \psi ds, \quad \forall \psi \in H^1(\Omega). \quad (4.4)$$

The imaginary part v_{im} of v satisfies

$$\begin{cases} -\Delta v_{im} + v_{im} = 0 & \text{in } \Omega, \\ \frac{\partial v_{im}}{\partial \mathbf{n}} + v_{re} = g_1^{\delta} - g_1 & \text{on } \Gamma, \end{cases}$$

whose weak form is

$$\int_{\Omega} (\nabla v_{im} \cdot \nabla \psi + v_{im} \psi) dx = \int_{\Gamma} (g_1^{\delta} - g_1) \psi ds - \int_{\Gamma} v_{re} \psi ds, \quad \forall \psi \in H^1(\Omega). \quad (4.5)$$

Set $\psi = v_{re}$ in (4.4) and $\psi = v_{im}$ in (4.5), and then add these two equations together to obtain

$$\|v_{re}\|_{1,\Omega}^2 + \|v_{im}\|_{1,\Omega}^2 = \int_{\Gamma} (g_2^{\delta} - g_2) v_{re} ds + \int_{\Gamma} (g_1^{\delta} - g_1) v_{im} ds,$$

which implies

$$\|v\|_{1,\Omega}^2 \leq \delta \int_{\Gamma} (|v_{re}| + |v_{im}|) ds. \quad (4.6)$$

On the other hand, if Ω is a ball/annulus in \mathbb{R}^d centered at 0 with radius R (and r), it holds (Motron (2002))

$$\int_{\Gamma} |u(s)| ds \leq \frac{d}{R} \int_{\Omega} |u(x)| dx + \int_{\Omega} |\nabla u(x)| dx \quad (4.7)$$

for all $u \in W^{1,1}(\Omega)$. Then, by inequality (4.7) and the Cauchy-Schwarz inequality $\int_{\Omega} |u(x)| dx \leq R\pi^{1/2} \|u\|_{0,\Omega}$, we deduce that for $k = re$ or im

$$\int_{\Gamma} |v_k| ds \leq d\pi^{1/2} \|v_k\|_{0,\Omega} + R\pi^{1/2} \|\nabla v_k\|_{0,\Omega} \leq \max(d, R)\pi^{1/2} \|v_k\|_{1,\Omega}. \quad (4.8)$$

Combine (4.6), (4.8), and the inequality $\|v_{re}\|_{1,\Omega} + \|v_{im}\|_{1,\Omega} \leq \sqrt{2} \|v\|_{1,\Omega}$ to obtain

$$\|u_{im}(p^{\dagger})\|_{0,\Omega} = \|v_{im}\|_{0,\Omega} \leq \|v\|_{1,\Omega} \leq \max(d, R)(2\pi)^{1/2} \delta,$$

which yields the required result. For the general smooth bounded domain, the proposition can be proven by using the Sobolev trace embedding inequality (with the constant S)

$$S \int_{\Gamma} |u(s)| ds \leq \int_{\Omega} |u(x)| + |\nabla u(x)| dx. \quad (4.9)$$

□

REMARK 4.1 The best (largest) embedding constant in (4.9) equals

$$S = \inf_{u \in W^{1,1}(\Omega)} \frac{\int_{\Omega} |u(x)| + |\nabla u(x)| dx}{\int_{\Gamma} |u(s)| ds}. \quad (4.10)$$

The extrema of (4.10) exists as the the embedding (4.9) is compact, cf. Fernandez Bonder & Rossi (2001). To the best of our knowledge, the rigorous lower bounds of S , hence the value of $C_0(\Omega)$ in

Proposition 4.1, for general smooth domain Ω is still open. Alternatively, one can estimate the value of S by numerically solving the following non-linear eigenvalue problem

$$\begin{cases} \operatorname{div} \left(\frac{\nabla u}{|\nabla u|} \right) = 1 & \text{in } \Omega, \\ \frac{\partial u}{\partial \mathbf{n}} = \lambda |\nabla u| & \text{on } \Gamma, \end{cases} \quad (4.11)$$

by noting that the extrema in (4.9) can be assumed positive, see e.g., Tolksdorf (1984); Vazquez (1984).

PROPOSITION 4.2 Let $p^\delta(x, t)$ be the dynamic solution of (2.6)-(2.8) with the fixed damping parameter $\eta \geq 1$ or $\eta(t) = r/t$ ($r > 3$). Then, $\lim_{t \rightarrow \infty} V(p^\delta(x, t)) \leq C_0^2 \delta^2$, where $V(\cdot)$ is defined in (2.2).

The proof of the above proposition is provided in the Appendix B. Now, we discuss the method of selecting the terminating time T^* . In this work, we consider the following two discrepancy functions:

- The Morozov's conventional discrepancy function:

$$\chi(T) = \|u_{im}(p^\delta(x, T))\|_{0, \Omega} - C_0 \tau \delta, \quad (4.12)$$

where $u = u_{re} + iu_{im}$ is the solution of (2.8) with noisy data, and τ is a fixed positive number.

- The total energy discrepancy function:

$$\chi_{TE}(T) = V(p^\delta(x, T)) + \|\dot{p}^\delta(x, T)\|_P^2 - C_0^2 \tau^2 \delta^2, \quad (4.13)$$

where $V(p^\delta) = \|u_{im}(p^\delta)\|_{0, \Omega}^2$.

LEMMA 4.1 Under the assumption $\tau > 1$, the following two assertions hold.

- If $\|u_{im}(p_0)\|_{0, \Omega} \geq C_0 \tau \delta$, then $\chi(T)$ has at least one root.
- If $V(p_0) + \|\dot{p}_0\|_P^2 \geq C_0^2 \tau^2 \delta^2$, then $\chi_{TE}(T)$ has a unique solution.

Proof. The continuity of $\chi(T)$ and $\chi_{TE}(T)$ are obviously according to Lemma 2.2 and Theorem 2.3. From Proposition 4.2 and the assumption of the lemma, we conclude that

$$\lim_{T \rightarrow \infty} \chi(T) \leq C_0(1 - \tau)\delta < 0 \text{ and } \lim_{T \rightarrow \infty} \chi_{TE}(T) \leq C_0^2(1 - \tau^2)\delta^2 < 0, \quad (4.14)$$

and $\chi(0) = \|u_{im}(p_0)\|_{0, \Omega} - C_0 \tau \delta > 0$ and $\chi_{TE}(0) = V(p_0) + \|\dot{p}_0\|_P^2 - C_0^2 \tau^2 \delta^2 > 0$, which implies the existence of the root of $\chi(T)$ and $\chi_{TE}(T)$.

The non-growing of $\chi_{TE}(T)$ is straightforward according to $\dot{\chi}_{TE} = -\eta \|\dot{p}^\delta\|_P^2$ for the fixed damping parameter and $\dot{\chi}_{TE} = -\frac{r}{T} \|\dot{p}^\delta\|_P^2$ for the dynamic damping parameter.

Finally, let us show that $\chi_{TE}(T)$ has a unique solution. We prove this by contradiction. Since $\chi_{TE}(T)$ is a non-increasing function, a number T_0 exists so that $\chi_{TE}(T) = 0$ for $T \in [T_0, T_0 + \varepsilon]$ with some positive $\varepsilon > 0$. This means that $\dot{\chi}_{TE}(T) = -\eta \|\dot{p}^\delta\|_P^2 \equiv 0$ (or $\dot{\chi}_{TE}(T) = -\frac{r}{T} \|\dot{p}^\delta\|_P^2 \equiv 0$) in $(T_0, T_0 + \varepsilon)$. Hence, $\dot{p}^\delta \equiv 0$ in $(T_0, T_0 + \varepsilon)$. Using the equation (1.9) we conclude that for all $T > T_0$: $p^\delta(T) \equiv p^\delta(T_0)$. Since $\chi_{TE}(T_0) = 0$, we obtain that $\chi_{TE}(T) \equiv 0$ for $T > T_0$, which implies that $\lim_{T \rightarrow \infty} \chi_{TE}(T) = 0$. This contradicts the fact in (4.14). \square

REMARK 4.2 It should be noted that Lemma 4.1 may still hold in the case $\tau \leq 1$. In many situations, e.g. for our numerical examples in Section 6, a small value of τ offers a better result, provided the existence of the root of χ or χ_{TE} .

THEOREM 4.3 (Convergence for noisy data) Let $p^\delta(x, t)$ be the dynamic solution of (2.6)-(2.8). Then, if the terminating time point T^* is selected as the root of $\chi(T)$ or $\chi_{TE}(T)$, $p^\delta(x, T^*(\delta))$ converges weakly to $p^\dagger(x)$ in P as $\delta \rightarrow 0$.

Proof. We use the technique from (Hanke *et al.*, 1995, Theorem 2.4). Let $\{\delta_n\}$ be a sequence converging to 0 as $n \rightarrow \infty$, and let $\{g_1^{\delta_n}, g_2^{\delta_n}\}$ be a corresponding sequence of noisy data with $\|g_1^{\delta_n} - g_1\|_{0,\Gamma} \leq \delta_n$ and $\|g_2^{\delta_n} - g_2\|_{0,\Gamma} \leq \delta_n$. For a triple $(\delta_n, g_1^{\delta_n}, g_2^{\delta_n})$, denote by $T_n^* = T^*(\delta_n)$ the corresponding terminating time point determined from the generalized discrepancy principles $\chi(T) = 0$ or $\chi_{TE}(T) = 0$.

Two possible cases exist. (i) T_n^* has a finite accumulation point T^* . (ii) $T_n^* \rightarrow \infty$ as $\delta_n \rightarrow 0$. For the case (i), without loss of generality we can assume that $T_n^* = T^*$ for all $n \in \mathbf{N}$. Hence, from the definition of T_n^* it follows that

$$\|u_{im}(p^{\delta_n}(\cdot, T_n^*))\|_{0,\Omega} \leq C_0 \tau \delta_n. \quad (4.15)$$

Since $p^{\delta_n}(\cdot, T_n^*)$ depends continuously on $\{g_1^{\delta_n}, g_2^{\delta_n}\}$ when T_n^* is fixed, we have

$$p^{\delta_n}(\cdot, T_n^*) \rightarrow p(\cdot, T^*), \quad \|u_{im}(p^{\delta_n}(\cdot, T_n^*))\|_{0,\Omega} \rightarrow \|u_{im}(p(\cdot, T^*))\|_{0,\Omega}. \quad n \rightarrow \infty, \quad (4.16)$$

where $p(\cdot, t)$ denotes the dynamic solution of (2.6)-(2.8) with noise-free data. Letting $n \rightarrow \infty$ in (4.15) yields $\|u_{im}(p(\cdot, T^*))\|_{0,\Omega} = 0$. Thus, $p(x, T^*) = p^\dagger(x)$, a solution of (1.1), and with (4.16) we obtain the strong convergence: $p(\cdot, T_n^*) \rightarrow p^\dagger(\cdot)$ in P as $n \rightarrow \infty$.

Now, consider the case (ii). According to the continuity of $p^{\delta_n}(\cdot, t)$, for any positive ε_0 and T_n^* , there exists a point $T^* < T_n^*$ such that

$$\|p^{\delta_n}(\cdot, T_n^*) - p^{\delta_n}(\cdot, T^*)\|_P \leq \varepsilon_0. \quad (4.17)$$

On the other hand, for any $q(\cdot) \in P$,

$$\begin{aligned} |(p^{\delta_n}(\cdot, T_n^*) - p^\dagger(\cdot), q(\cdot))_P| &\leq \\ |(p^{\delta_n}(\cdot, T_n^*) - p^{\delta_n}(\cdot, T^*), q(\cdot))_P| &+ |(p^{\delta_n}(\cdot, T^*) - p(\cdot, T^*), q(\cdot))_P| + |p(\cdot, T^*) - p^\dagger(\cdot), q(\cdot))_P|. \end{aligned}$$

By inequality (4.17) and the weak convergence of $p(\cdot, t)$, one can fix T^* so large that both inequalities $|(p^{\delta_n}(\cdot, T_n^*) - p^{\delta_n}(\cdot, T^*), q(\cdot))_P| \leq \varepsilon/3$ and $|p(\cdot, T^*) - p^\dagger(\cdot), q(\cdot))_P| \leq \varepsilon/3$ hold. Now that T^* is fixed, we can apply the result of case (i) to conclude that a positive number $n_1 = n_1(T^*)$ exists such that for any $n \geq n_1$: $|(p^{\delta_n}(\cdot, T^*) - p(\cdot, T^*), q(\cdot))_P| \leq \varepsilon/3$. Combine the above inequalities to obtain $|(p^{\delta_n}(\cdot, T_n^*) - p^\dagger(\cdot), q(\cdot))_P| \leq \varepsilon$ for all $n \geq n_1$. Since ε is arbitrary, we complete the proof. \square

5. Full discretization and a novel iterative regularization algorithm

5.1 Space discretization

Following Johnson (2009), we discretize the bounded domain Ω by mesh \mathcal{T} using non-overlapping triangles/tetrahedrons $\{\Delta_\mu\}_{\mu=1}^M$. We associate the mesh \mathcal{T} with the mesh function $h(x)$, which is a piecewise-constant function such that $h(x) \equiv \ell(\Delta_\mu)$ for all $x \in \Delta_\mu$, where $\ell(\Delta_\mu)$ is the longest side of $\Delta_\mu \in \mathcal{T}$. Define the mesh scale size as $h := \max_{x \in \Omega} h(x)$. Let $r(\Delta_\mu)$ be the radius of the maximal circle/ball contained in the triangle/tetrahedron Δ_μ . We make the following shape regularity assumption for every element $\Delta_\mu \in \mathcal{T}$: $c_1 \leq \ell(\Delta_\mu) \leq c_2 r(\Delta_\mu)$, where c_1 and c_2 are two positive constants. Now, we introduce the finite element space

$$\Psi^h = \{v \in C(\Omega) : v \in \mathcal{P}_1(\Delta_\mu) \text{ for all } \Delta_\mu \in \mathcal{T}\}, \quad (5.1)$$

where $\mathcal{P}_1(\Delta_\mu)$ denotes the set of all linear continuous functions on Δ_μ .

Denote $\Psi^h := \Psi^h \oplus i\Psi^h$. Then, Ψ^h is a finite element subspace of $\mathbf{H}^1(\Omega)$, and the finite element approximation of the BVP (2.9) is as follows:

$$\text{find } u^h \in \Psi^h \text{ such that } a(u^h, \psi^h) = f^\delta(\psi^h), \quad \forall \psi^h \in \Psi^h. \quad (5.2)$$

The problem (5.2) admits a unique solution $u^h \in \Psi^h$ according to Lemma 2.1. Similar to those in Cheng *et al.* (2014), it is not difficult to derive the following a priori finite element error estimates.

THEOREM 5.1 Let $u \in \mathbf{H}^1(\Omega)$ be the solution of the problem (2.9) and $u^h \in \Psi^h$ be the finite element solution of problem (5.2) respectively. Then, for any $p(\cdot, t) \in L^2((t_0, \infty), P)$ and almost every $t > 0$

$$\|u^h(p(\cdot, t)) - u(p(\cdot, t))\|_{1, \Omega} \leq C(\Omega)h \left(\|p(\cdot, t)\|_{0, \Omega_0} + \|g_1^\delta\|_{0, \Gamma} + \|g_2^\delta\|_{0, \Gamma} \right).$$

Note that, in this section, we set $t_0 = 0$ or 1, corresponding to the model (2.6) with different damping parameter $\eta(t) = \text{const.}$ or r/t . Now we are in a position to discretize the second order evolution equation (2.6). For this purpose, set $P^h = P \cap \Psi^h$ and the orthogonal projection operator $\Pi^h : P \rightarrow P^h$

$$(\Pi^h p, q^h)_{k, \Omega_0} = (p, q^h)_{k, \Omega_0}, \quad \forall p \in P, q^h \in P^h, k = 0, 1. \quad (5.3)$$

Then for all $p \in H^{k+1}(\Omega_0)$ (Atkinson & Han, 2009, Theorem 10.3.8):

$$\|\Pi^h p - p\|_{m, \Omega_0} \leq C(\Omega)h^{k+1-m} |p|_{k+1, \Omega_0}, \quad m = 0, 1. \quad (5.4)$$

Introduce a discrete optimization problem

$$\min_{p \in P^h} V_h(p) = \min_{p \in P^h} \frac{1}{2} \|u_{im}^h(p)\|_{0, \Omega}^2, \quad (5.5)$$

where $u^h = u_{re}^h + iu_{im}^h \in \Psi^h$ is the weak solution of the problem (5.2), and a semi-discretized second order flow

$$\begin{cases} \ddot{p}^{\delta, h}(x, t) + \eta(t)\dot{p}^{\delta, h}(x, t) + w_{im}^h(x, t) = 0, & x \in \Omega_0, t \in (t_0, \infty), \\ p^{\delta, h}(x, t_0) = p_0^h, \dot{p}^{\delta, h}(x, t_0) = \dot{p}_0^h, & x \in \Gamma, t \in (t_0, \infty), \end{cases} \quad (5.6)$$

where p_0^h and \dot{p}_0^h are projections of p_0 and \dot{p}_0 in P^h , w^h is the finite element solution to the joint problem

$$\begin{cases} -\Delta w(x, t) + cw(x, t) = u_{im}^h(p^{\delta, h}(x, t)), & x \in \Omega_0, t \in (t_0, \infty), \\ \frac{\partial w(x, t)}{\partial \mathbf{n}} + iw(x, t) = 0, & x \in \Gamma, t \in (t_0, \infty), \end{cases} \quad (5.7)$$

and $u_{im}^h(p^{\delta, h}(x, t))$ is the imaginary part of the solution of (5.2), with p^δ replaced by $p^{\delta, h}$.

PROPOSITION 5.2 Let $w^\delta \in \mathbf{H}^1(\Omega)$ be the weak solution of (2.9) with $p^\delta(\cdot, t)$ replaced by $p^{\delta, h}(\cdot, t)$, and $w^{\delta, h} \in \Psi^h$ be the finite element solution of (5.7). Then, a constant $C(\Omega)$ exists such that for any $p^{\delta, h}(\cdot, t) \in L^2((t_0, \infty), P^h)$, and almost every $t \in [t_0, \infty)$,

$$\|w^{\delta, h}(p^{\delta, h}(\cdot, t)) - w^\delta(p^{\delta, h}(\cdot, t))\|_{1, \Omega} \leq C(\Omega)h \left(\|p^{\delta, h}(\cdot, t)\|_{0, \Omega_0} + \|g_1^\delta\|_{0, \Gamma} + \|g_2^\delta\|_{0, \Gamma} \right).$$

Combining Theorems 2.3 and 5.1, Proposition 5.2, as well as the definition of Π^h , it is not difficult to obtain the following estimate.

PROPOSITION 5.3 Let $p^\delta(\cdot, t) \in P$ and $p^{\delta,h}(\cdot, t) \in P^h$ be solutions of (2.6) and (5.6) respectively. Then, a constant $C(\Omega)$ exists such that for almost every $t \in [t_0, \infty)$,

$$\|p^{\delta,h}(\cdot, t) - p^\delta(\cdot, t)\|_P \leq C(\Omega)h \left(\|g_1^\delta\|_{0,\Gamma} + \|g_2^\delta\|_{0,\Gamma} \right).$$

Now, we present the main result in this subsection.

THEOREM 5.4 (convergence of the finite element solution) Let $p^{\delta,h} \in P^h$ be solution of (5.6). Suppose that for almost every $t > 0$ and $\delta \geq 0$, $p^\delta(\cdot, t) \in H^1(\Omega_0)$. Then, under the assumption of Theorem 4.3, we have the strong convergence, i.e., $p^{\delta,h}(\cdot, T^*(\delta)) \rightarrow p^\dagger(\cdot)$ in $L^2(\Omega_0)$ as $\delta, h \rightarrow 0$.

Proof. By the triangle inequality

$$\begin{aligned} \|p^{\delta,h}(\cdot, T^*(\delta)) - p^\dagger(\cdot)\|_{0,\Omega_0} &\leq \|p^{\delta,h}(\cdot, T^*(\delta)) - p^\delta(\cdot, T^*(\delta))\|_{0,\Omega_0} + \\ &\|p^\delta(\cdot, T^*(\delta)) - \Pi^h p^\delta(\cdot, T^*(\delta))\|_{0,\Omega_0} + \|\Pi^h p^\delta(\cdot, T^*(\delta)) - \Pi^h p^\dagger(\cdot)\|_{0,\Omega_0} + \|\Pi^h p^\dagger(\cdot) - p^\dagger(\cdot)\|_{0,\Omega_0}, \end{aligned}$$

it suffices to show the convergence of all terms in the right-hand side of the above inequality. The convergence of the first term follows from Proposition 5.3, while the second and fourth terms converge to 0 because of the inequality (5.4). Finally, the convergence of the third term follows from Theorem 4.3 and the assertion (b) of Remark 3.3. \square

Finally, we give a sketch of the finite element method for problems (2.7) and (2.8). For conciseness, by slightly abusing the notation, we rewrite $p^{\delta,h}$, $\dot{p}^{\delta,h}$ and $\ddot{p}^{\delta,h}$ to p^h , \dot{p}^h and \ddot{p}^h . Let m be the number of the nodes of triangulation \mathcal{T} , and $\{\psi_l\}_{l=1}^m$ be the nodal basis functions of the linear finite element space Ψ^h associated with the grid points $\{x_l\}_{l=1}^m$. Then $u^h(x, t) = \sum_{l=1}^m u_l(t) \psi_l(x)$ with $u_l(t) = u^h(x_l, t) \in L^2((t_0, \infty), \mathbb{C})$ and $w^h(x, t) = \sum_{l=1}^m w_l(t) \psi_l(x)$ with $w_l(t) = w^h(x_l, t) \in L^2((t_0, \infty), \mathbb{C})$. Denote $\{x_{k_l}\}_{l=1}^{m_0} = \{x_l\}_{l=1}^m \cap \overline{\Omega}_0$, $p^h(x, t) = \sum_{l=1}^{m_0} p_l(t) \psi_{k_l}(x)$ with $p_l(t) = p^h(x_{k_l}, t) \in L^2((t_0, \infty), \mathbb{R})$. As a result, the problem (5.2) reduces to the following algebraic system with any fixed t :

$$\begin{cases} (D+E)\mathbf{u}_{re}(t) - F\mathbf{u}_{im}(t) = B\mathbf{p}(t) + \mathbf{b}_2, \\ F\mathbf{u}_{re}(t) + (D+E)\mathbf{u}_{im}(t) = \mathbf{b}_1, \end{cases} \quad (5.8)$$

where

$$\begin{aligned} D &= [d_{ls}]_{m \times m}, d_{ls} = \int_{\Omega} \nabla \psi_s \cdot \nabla \psi_l dx, & E &= [e_{ls}]_{m \times m}, e_{ls} = \int_{\Omega} \psi_s \psi_l dx, \\ F &= [f_{ls}]_{m \times m}, f_{ls} = \int_{\Gamma} \psi_s \psi_l ds, & B &= [b_{lj}]_{m \times m_0}, b_{lj} = \int_{\Omega_0} \psi_l(x) \psi_{k_j}(y) dx, \\ \mathbf{b}_1 &= [b_{1,l}]_{m \times 1}, b_{1,l} = \int_{\Gamma} g_1^\delta \psi_l ds, & \mathbf{b}_2 &= [b_{2,l}]_{m \times 1}, b_{2,l} = \int_{\Gamma} g_2^\delta \psi_l ds, \\ \mathbf{u}_{re} &= [u_{re,l}]_{m \times 1}, \mathbf{u}_{im} = [u_{im,l}]_{m \times 1}, \mathbf{p} = [p_j]_{m_0 \times 1}, & l, s &= \overline{1, m}, j = \overline{1, m_0}. \end{aligned}$$

Similarly, for any fixed t , finding a weak solution of (5.7) reduces to solve the following system of linear equations

$$\begin{cases} (D+E)\mathbf{w}_{re}(t) - F\mathbf{w}_{im}(t) = E\mathbf{u}_{im}(t), \\ F\mathbf{w}_{re}(t) + (D+E)\mathbf{w}_{im}(t) = \mathbf{0}. \end{cases} \quad (5.9)$$

5.2 Time discretization and a novel iterative regularization algorithm

The second order evolution equation (2.6) with an appropriate numerical discretization scheme for the artificial time variable yields a concrete second order iterative regularization method. The damped

symplectic integrators are extremely attractive for solving second order systems, since the schemes are closely related to the canonical transformations (Hairer *et al.* (2006)), and the trajectories of the discretized second flow usually kept some intrinsic invariants of the system. In this paper, we use the Störmer-Verlet method, which belongs to the family of symplectic integrators.

Denote $q^h(x, t) = \dot{p}^h(x, t)$, and rewrite (5.6) into the first order system

$$\begin{cases} \dot{q}^h = -\eta q^h - w_{im}^h \chi_{\Omega_0}, \\ \dot{p}^h = q^h, \\ p^h(t_0) = p_0^h, q^h(t_0) = \dot{p}_0^h. \end{cases} \quad (5.10)$$

Apply the Störmer-Verlet method to the system (5.10) to obtain that at the k -th iteration

$$\begin{cases} q_{k+\frac{1}{2}}^h = q_k^h - \frac{\Delta t}{2} (\eta_k q_k^h + w_{im}^h(p_k^h) \chi_{\Omega_0}), \\ p_{k+1}^h = p_k^h + \Delta t q_{k+\frac{1}{2}}^h, \\ q_{k+1}^h = q_{k+\frac{1}{2}}^h - \frac{\Delta t}{2} (\eta_{k+1} q_{k+\frac{1}{2}}^h + w_{im}^h(p_{k+1}^h) \chi_{\Omega_0}), \\ q^h(t_0) = \dot{p}_0^h, p^h(t_0) = p_0^h, \end{cases} \quad (5.11)$$

where $p_k^h = p^{\delta, h}(t_k)$, and Δt is the time step size.

Taking into account of the discrepancy principle for choosing the terminating time point, the newly developed numerical algorithm is proposed as follows:

Algorithm 1 The Störmer-Verlet based SOAR for inverse source problem (1.1).

Require: Boundary data $\{g_1^\delta, g_2^\delta\}$. Noise level δ . Damping parameter $\eta(t)$. Time step size Δt . The permissible region Ω_0 . Triangulation \mathcal{T} of domain Ω with the nodal basis functions $\{\psi_i\}_{i=1}^m$.

Precision number ε_0 . Initial values: $(\mathbf{p}^0, \mathbf{q}^0)$. Iteration index: $k \leftarrow 0$.

Ensure: The estimated source term: $\hat{p}^h = \sum_{l=1}^{m_0} \mathbf{p}_l^k \psi_{k_l}$.

- 1: **while** $\chi(t_k) > \varepsilon_0$ or $\chi_{TE}(t_k) > \varepsilon_0$ **do**
 - 2: Solve (5.8) and (5.9) with source \mathbf{p}^k to get \mathbf{w}_{im}^k .
 - 3: $\mathbf{q}^{k+\frac{1}{2}} \leftarrow \mathbf{q}^k - \frac{\Delta t}{2} (\eta_k \mathbf{q}^k + \mathbf{w}_{im}^k)$
 - 4: $\mathbf{p}^{k+1} \leftarrow \mathbf{p}^k + \Delta t \mathbf{q}^{k+\frac{1}{2}}$
 - 5: Solve (5.8) and (5.9) with source \mathbf{p}^{k+1} to get \mathbf{w}_{im}^{k+1} .
 - 6: $\mathbf{q}^{k+1} \leftarrow \mathbf{q}^{k+\frac{1}{2}} - \frac{\Delta t}{2} (\eta_{k+1} \mathbf{q}^{k+\frac{1}{2}} + \mathbf{w}_{im}^{k+1})$
 - 7: $t_{k+1} \leftarrow t_k + \Delta t$
 - 8: $k \leftarrow k + 1$
 - 9: **end while**
-

6. Simulations

In this section, we present some numerical examples to demonstrate the effectiveness of the proposed second order asymptotical regularization (SOAR) methods. With the problem domain Ω , Neumann data g_2 , and a prescribed true source function p^\dagger in $\Omega_0 \subset \Omega$, by using the standard linear finite element method defined in Subsection 5.1, we solve the forward BVP

$$-\Delta u + u = p^\dagger \chi_{\Omega_0} \text{ in } \Omega, \text{ and } \frac{\partial u}{\partial \mathbf{n}} = g_2 \text{ on } \Gamma \quad (6.1)$$

to get $u^h \in \Psi^h$. Use $g_1 = u^h|_\Gamma$ for the boundary measurement. Uniformly distributed noises with the relative error level δ' are added to both g_1 and g_2 to get g_1^δ and g_2^δ :

$$g_j^\delta(x) = [1 + \delta' \cdot (2\text{rand}(x) - 1)]g_j(x), \quad x \in \Gamma, \quad j = 1, 2,$$

where $\text{rand}(x)$ returns a pseudo-random value drawn from a uniform distribution on $[0, 1]$. The noise level of measurement data is calculated by $\delta = \max_{j=1,2} \|g_j^\delta - g_j\|_{\infty, \Gamma}$. Then, with the noisy data g_1^δ and g_2^δ , properly chosen parameters, e.g. η and Δt , **Algorithm 1** is implemented to get p^h – a stable approximation of p^\dagger by SOAR. In all experiments below, we set $g_2 \equiv 0$ on Γ , $t_0 = 1$ and the precision parameter $\varepsilon_0 = 10^{-6}$. We use N_{max} as the maximal number of iterations where **Algorithm 1** stops, which may have different values in different experiments.

We refer to SOAR1 as **Algorithm 1** when η is constant and χ is used; SOAR2 when η is constant and χ_{TE} is used; SOAR3 when $\eta = r/t$ and χ is used; SOAR4 when $\eta = r/t$ and χ_{TE} is used. To assess the accuracy of the approximate solutions, we define the L^2 -norm relative error for an approximate solution p^h : $\text{L2Err} := \|p^h - p^\dagger\|_{0, \Omega} / \|p^\dagger\|_{0, \Omega}$. All experiments in Subsection 6.1–6.3 are implemented for the following two examples:

Example 1: $\Omega := \{(x_1, x_2) \in \mathbb{R}^2 | x_1^2 + x_2^2 < 1\}$, $\Omega_0 := \{(x_1, x_2) \in \mathbb{R}^2 | -0.5 < x_1, x_2 < 0.5\}$. $p^\dagger(x_1, x_2) = (1 + x_1 + x_2)\chi_{\Omega_0}$. The Dirichlet data g_1 is computed on a mesh with mesh size $h = 0.01386$, 144929 nodes and 288768 elements.

Example 2: Ω is the same as Example 1. $\Omega_0 = \Omega_1 \cup \Omega_2$ with $\Omega_1 := \{(x_1, x_2) \in \mathbb{R}^2 | (x_1 + 0.5)^2 + x_2^2 < 0.01\}$ and $\Omega_2 := \{(x_1, x_2) \in \mathbb{R}^2 | (x_1 - 0.5)^2 + x_2^2 < 0.01\}$. $p^\dagger(x_1, x_2) = (1 + x_1 + x_2)\chi_{\Omega_1} + e^{1+x_1+x_2}\chi_{\Omega_2}$. The Dirichlet data g_1 is computed on a mesh with $h = 0.01228$, 156225 nodes and 311296 elements.

For Example 1, all approximate sources are reconstructed over a mesh with mesh size $h = 0.1293$, 599 nodes and 1128 elements. For Example 2, all approximate sources are reconstructed over a mesh with mesh size $h = 0.1222$, 645 nodes and 1216 elements.

6.1 Regularization of the method

We first validate the convergence result of Theorem 4.3. **Algorithm 1** is implemented for $\delta' = 2^{-1}, 2^{-2}, \dots, 2^{-15}$. As indicated by the assumptions of Lemma 4.1 and Theorem 4.3, let $\tau = 1.1$ (used in

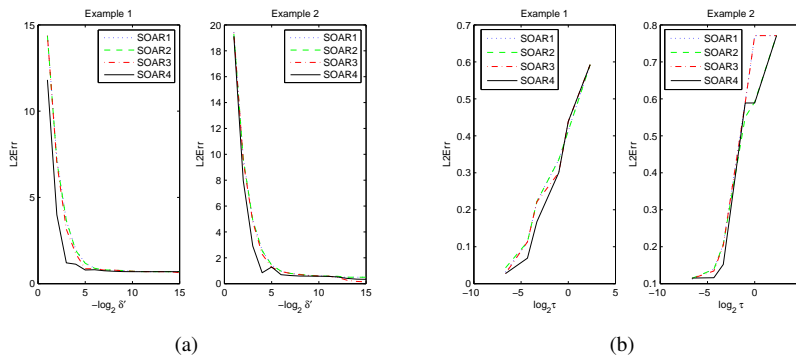


FIG. 1. (a) Evolutions of L2Err vs. δ' . (b) Evolutions of L2Err vs. τ with $\Delta t = 10, \eta = 0.1$ or $5/t$.

(4.12) and (4.13)), $\eta = 1$ when it is constant, $\eta = 5/t$ when it is dynamic, $p_0 = 30, q_0 = \dot{p}_0 = 0$ in Ω_0 for Example 1, and $p_0 = 70, q_0 = \dot{p}_0 = 0$ in Ω_0 for Example 2 so that (p_0, \dot{p}_0) satisfies $\|u_{im}(p_0)\|_{0,\Omega} > C_0\tau\delta$ and $V(p_0) + \|\dot{p}_0\|_p^2 > C_0^2\tau\delta^2$ ($C_0 = 2\sqrt{2\pi}$). Moreover, for the implementation of **Algorithm 1**, set the time step $\Delta t = 1$.

The evolutions of L2-norm relative errors in approximate solutions computed from **Algorithm 1** are plotted in (a) of Figure 1, which indicates that **Algorithm 1** for all four cases are convergent and, thus confirms the theoretical analysis. The detailed errors and the corresponding iterative numbers are given in Tables 1 and 2, where we can see that for both examples, using a dynamic damping parameter $\eta(t)$ and the total energy discrepancy functional χ_{TE} can accelerate the iteration, and this is particularly remarkable when the noise level δ' is relatively small. However, as shown in Figure 1(a) and Tables 1 and 2, compared with the noise level δ , the accuracy of the obtained approximate solution is not highly qualified. This is because the iterations stop before getting satisfactory approximate solutions. As mentioned in Remark 4.2, constants $\eta \geq 1$ and $\tau > 1$ are just the sufficient conditions for Lemmas 3.1 and 4.1. As we shall see in the next subsection, using smaller values of the parameters η and τ will

δ'	SOAR1		SOAR2	
	L2Err	IterNum	L2Err	IterNum
2^{-1}	14.3642	21	14.3642	21
2^{-2}	7.3013	43	7.0815	44
2^{-3}	3.6594	66	3.6594	66
2^{-4}	1.9695	88	1.9190	89
2^{-5}	1.1803	111	1.1803	111
2^{-6}	0.8950	133	0.8881	134
2^{-7}	0.8021	156	0.8002	157
2^{-8}	0.7744	182	0.7744	182
2^{-9}	0.7638	226	0.7638	226
2^{-10}	0.7171	957	0.7178	936
2^{-11}	0.7004	1835	0.7012	1754
2^{-12}	0.6961	2723	0.6969	2441
2^{-13}	0.6950	3650	0.6958	2868
2^{-14}	0.6946	4790	0.6955	3043
2^{-15}	0.6918	N_{max}	0.6955	3095
δ'	SOAR3		SOAR4	
	L2Err	IterNum	L2Err	IterNum
2^{-1}	14.3728	14	11.8109	16
2^{-2}	7.0005	20	3.9916	23
2^{-3}	3.1556	24	1.2075	27
2^{-4}	1.7341	26	1.1257	31
2^{-5}	0.8636	28	0.7910	46
2^{-6}	0.8637	28	0.8056	61
2^{-7}	0.7870	29	0.7453	80
2^{-8}	0.7871	29	0.7165	102
2^{-9}	0.7484	66	0.6993	137
2^{-10}	0.7162	102	0.6948	175
2^{-11}	0.6989	138	0.6949	228
2^{-12}	0.6958	156	0.6945	283
2^{-13}	0.6948	174	0.6944	321
2^{-14}	0.6945	282	0.6943	339
2^{-15}	0.6302	3829	0.6943	350

Table 1. Example 1: L2Err and IterNum vs δ' with $\tau = 1.1, \Delta t = 1, \eta = 1$ or $5/t, N_{max} = 50000$.

significantly improve the solution accuracy.

δ'	SOAR1		SOAR2	
	L2Err	IterNum	L2Err	IterNum
2^{-1}	19.4452	9	19.2942	10
2^{-2}	9.7309	98	9.6558	99
2^{-3}	4.9134	187	4.9134	187
2^{-4}	2.5508	276	2.5508	276
2^{-5}	1.4386	365	1.4386	365
2^{-6}	0.9641	456	0.9611	457
2^{-7}	0.7870	554	0.7870	554
2^{-8}	0.7181	690	0.7181	690
2^{-9}	0.6344	1423	0.6349	1416
2^{-10}	0.5912	2615	0.5917	2586
2^{-11}	0.5786	4085	0.5793	3915
2^{-12}	0.4981	N_{max}	0.5656	10262
2^{-13}	0.4981	N_{max}	0.4981	N_{max}
2^{-14}	0.4981	N_{max}	0.4981	N_{max}
2^{-15}	0.4981	N_{max}	0.4981	N_{max}
δ'	SOAR3		SOAR4	
	L2Err	IterNum	L2Err	IterNum
2^{-1}	19.3905	9	19.1197	10
2^{-2}	9.4475	32	7.9659	35
2^{-3}	4.7961	42	2.9125	47
2^{-4}	2.2760	49	0.8393	56
2^{-5}	1.2621	53	1.2887	67
2^{-6}	0.9376	55	0.6924	95
2^{-7}	0.7884	57	0.6254	129
2^{-8}	0.6978	93	0.5864	167
2^{-9}	0.6223	130	0.5804	222
2^{-10}	0.5869	165	0.5714	300
2^{-11}	0.5792	201	0.5585	409
2^{-12}	0.4749	873	0.5187	658
2^{-13}	0.2628	1714	0.4033	1171
2^{-14}	0.1703	2165	0.3491	1379
2^{-15}	0.1372	2451	0.3343	1435

Table 2. Example 2: L2Err and IterNum vs δ' with $\tau = 1.1, \Delta t = 1, \eta = 1$ or $5/t, N_{max} = 50000$.

6.2 Influence of parameters

The purpose of this subsection is to explore the dependence of the solution accuracy and the convergence speed on $\tau > 0$, time step size Δt , damping parameter η when it is constant or r when $\eta(t) = r/t$, and thus to give a guide on the choices of them in practice. For focusing on the effect of these parameters on **Algorithm 1**, we fix $\delta' = 5\%$ in this subsection. Moreover, in the remaining part of this section, we simply set $p_0 = q_0 = 0$. In addition, because the parameter τ does not involve the computation of the approximate solutions itself and only affects the iterative number where **Algorithm 1** stops, in the following, by slightly abusing the notation, we refer τ as $C_0\tau$.

We first investigate the influence of parameter τ on the convergence rate. For this purpose, we additionally set $\Delta t = 10, \eta = 0.1$ when η is constant or $\eta = 5/t$ when η is dynamic. The detailed L2-norm relative errors 'L2Err' and the corresponding iterative numbers 'IterNum' for different values of τ are

shown in Tables 3 and 4, which show that on one hand, the smaller τ is, the better the solution accuracy is; on the other hand, the smaller τ is, the more the iterative number for stopping **Algorithm 1** is. It is no surprise that the parameter τ does not involve the computation of the approximate solutions itself. It is used in stop criterion and only affects the iterative number where **Algorithm 1** stops. Therefore, it is natural that a larger iterative number produces a better approximate solution, and this also confirms the asymptotical behavior of the proposed method. The evolutions of L2Err vs. τ for both examples and four cases of **Algorithm 1** are plotted in (b) of Figure 1. Generally, $\tau < 1$ is enough to produce reasonable approximate solutions. Note that, as shown in Subsection 6.1, bigger τ may produce satisfactory approximate solutions when the noise level δ is rather small.

τ	SOAR1		SOAR2	
	L2Err	IterNum	L2Err	IterNum
0.01	0.0312	35	0.0429	28
0.05	0.1131	15	0.1131	15
0.1	0.2223	7	0.2223	7
0.5	0.3355	3	0.3355	3
1	0.4134	2	0.4134	2
5	0.5925	1	0.5925	1
τ	SOAR3		SOAR4	
	L2Err	IterNum	L2Err	IterNum
0.01	0.0274	19	0.0274	19
0.05	0.1131	12	0.0689	14
0.1	0.2212	8	0.1673	10
0.5	0.3006	6	0.3006	6
1	0.4388	4	0.4388	4
5	0.5925	1	0.5925	1

Table 3. Example 1: L2Err and IterNum vs τ with $\Delta t = 10, \eta = 0.1$ or $5/t$.

τ	SOAR1		SOAR2	
	L2Err	IterNum	L2Err	IterNum
0.01	0.1123	58	0.1143	49
0.05	0.1391	31	0.1391	31
0.1	0.2065	20	0.2065	20
0.5	0.5914	2	0.5504	3
1	0.7709	1	0.5914	2
5	0.7709	1	0.7709	1
τ	SOAR3		SOAR4	
	L2Err	IterNum	L2Err	IterNum
0.01	0.1137	20	0.1150	29
0.05	0.1342	17	0.1159	19
0.1	0.2037	14	0.1519	16
0.5	0.5887	2	0.5887	2
1	0.7709	1	0.5887	2
5	0.7709	1	0.7709	1

Table 4. Example 2: L2Err and IterNum vs τ with $\Delta t = 10, \eta = 0.1$ or $5/t$.

Now we investigate the influence of time step size Δt on the solution accuracy and the convergence rate. To this end, set $\tau = 0.01, \eta = 0.1$ or $5/t$. The L2-norm relative errors 'L2Err' and the corresponding iterative numbers 'IterNum' for both examples and four algorithms are given in Tables 5 and 6,

which show that the bigger the time step size Δt is, the faster the iteration is. However, our experiments suggest that Δt should not be too big. Otherwise, the iteration will blow up as it breaks the consistency of the numerical scheme. The evolutions of L2Err vs. Δt are plotted in Figure 2. In the remaining experiments, we choose $\Delta t = 10$.

Δt	SOAR1		SOAR2	
	L2Err	IterNum	L2Err	IterNum
0.01	0.3859	N_{max}	0.3859	N_{max}
0.05	0.2709	N_{max}	0.2709	N_{max}
0.1	0.1758	N_{max}	0.1758	N_{max}
0.5	0.0322	677	0.0432	556
1	0.0322	339	0.0433	278
5	0.0317	69	0.0430	56
10	0.0312	35	0.0429	28
Δt	SOAR3		SOAR4	
	L2Err	IterNum	L2Err	IterNum
0.01	0.7744	N_{max}	0.7744	N_{max}
0.05	0.3478	N_{max}	0.3178	N_{max}
0.1	0.1800	N_{max}	0.1800	N_{max}
0.5	0.0313	332	0.0260	363
1	0.0313	166	0.0261	182
5	0.0284	34	0.0258	36
10	0.0274	19	0.0274	19

Table 5. Example 1: L2Err and IterNum vs Δt with $\tau = 0.01, \eta = 0.1$ or $5/t, N_{max} = 1000$.

Δt	SOAR1		SOAR2	
	L2Err	IterNum	L2Err	IterNum
0.01	0.8353	N_{max}	0.8353	N_{max}
0.05	0.5027	N_{max}	0.5027	N_{max}
0.1	0.3616	N_{max}	0.3616	N_{max}
0.5	0.1123	N_{max}	0.1145	965
1	0.1123	576	0.1145	483
5	0.1123	116	0.1145	97
10	0.1123	58	0.1143	49
Δt	SOAR3		SOAR4	
	L2Err	IterNum	L2Err	IterNum
0.01	0.9521	N_{max}	0.9521	N_{max}
0.05	0.5570	N_{max}	0.5570	N_{max}
0.1	0.3691	N_{max}	0.3691	N_{max}
0.5	0.1137	396	0.1134	615
1	0.1137	198	0.1134	307
5	0.1138	40	0.1142	60
10	0.1137	20	0.1150	29

Table 6. Example 2: L2Err and IterNum vs Δt with $\tau = 0.01, \eta = 0.1$ or $5/t, N_{max} = 1000$.

We next discuss the influence of the damping parameter η on the solution accuracy and the convergence rate. In the experiments, set $\tau = 0.01, \Delta t = 10$. For constant η , the L2-norm relative errors 'L2Err' and the corresponding iterative numbers 'IterNum' are given in Tables 7 and 8 from which we conclude that $\eta \leq 0.1$ can lead to reasonable approximate solutions for **Algorithm 1** for four cases.

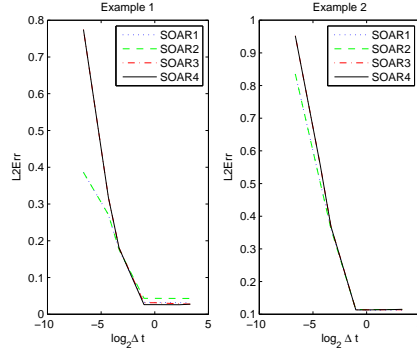


FIG. 2. Evolutions of L2Err vs. Δt with $\tau = 0.01, \eta = 0.1$ or $5/t$.

Nevertheless, η should not be too small. Too small η brings oscillation in solution accuracy. The evolutions of L2Err vs. η are shown in Figure 3. For dynamic damping parameter $\eta = r/t$, the L2-norm relative errors 'L2Err' and the corresponding iterative numbers 'IterNum' are given in Tables 7 and 8. The evolutions of 'L2Err' vs. the factor r are also shown in Figure 3. Both Tables 7, 8 and Figure 3 indicate that, like η , the factor r should be neither too small nor too big. Too small r also brings oscillation in solution accuracy. Therefore, in the remaining experiments, set $\eta = 0.05$ when it is constant while set $r = 5$ when $\eta = r/t$.

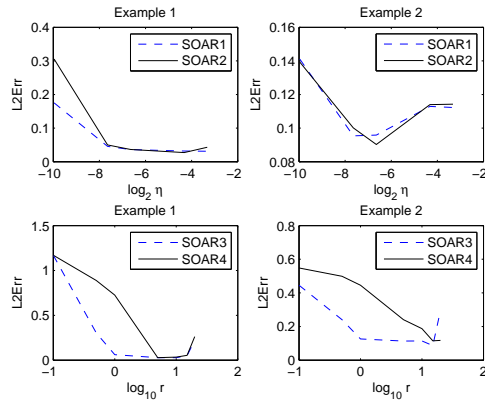


FIG. 3. Evolutions of L2Err vs. η with $\tau = 0.01, \Delta t = 10$.

Finally, we discuss the choice of the initial data (p_0, \dot{p}_0) for SOAR. According to the numerical experiments (for the concision of the statement, we omit the related numerical results), in most cases, the initial data (p_0, \dot{p}_0) does not effect the result quality (the value of "L2Err"), but may influence the algorithm speed. The closer the initial data (p_0, \dot{p}_0) is to the unknown exact solution, the less of the iteration number "IterNum" is required. Without knowledge of the exact solution, we recommend to set

$\eta = const.$	SOAR1		SOAR2	
	L2Err	IterNum	L2Err	IterNum
$\eta = 0.001$	0.1752	395	0.3057	849
$\eta = 0.005$	0.0455	97	0.0499	171
$\eta = 0.01$	0.0360	52	0.0365	87
$\eta = 0.05$	0.0316	14	0.0270	17
$\eta = 0.1$	0.0312	35	0.0429	28
$\eta = r/t$	SOAR3		SOAR4	
	L2Err	IterNum	L2Err	IterNum
$r = 0.1$	1.1695	N_{max}	1.1695	N_{max}
$r = 0.5$	0.3030	440	0.8882	N_{max}
$r = 1$	0.0616	131	0.7251	N_{max}
$r = 5$	0.0274	19	0.0274	19
$r = 10$	0.0280	26	0.0343	23
$r = 15$	0.0503	40	0.0536	43
$r = 20$	0.2220	153	0.2622	139

Table 7. Example 1: L2Err and IterNum vs $\eta = const.$ or r/t with $\tau = 0.01, \Delta t = 10, N_{max} = 1000$.

$\eta = const.$	SOAR1		SOAR2	
	L2Err	IterNum	L2Err	IterNum
$\eta = 0.001$	0.1410	208	0.1393	885
$\eta = 0.005$	0.0954	118	0.1001	176
$\eta = 0.01$	0.0958	49	0.0903	87
$\eta = 0.05$	0.1129	25	0.1140	22
$\eta = 0.1$	0.1123	58	0.1143	49
$\eta = r/t$	SOAR3		SOAR4	
	L2Err	IterNum	L2Err	IterNum
$r = 0.1$	0.4453	N_{max}	0.4453	N_{max}
$r = 0.5$	0.2407	N_{max}	0.2407	N_{max}
$r = 1$	0.1261	136	0.1875	N_{max}
$r = 5$	0.1137	20	0.1150	29
$r = 10$	0.1146	25	0.1175	22
$r = 15$	0.0863	46	0.0868	56
$r = 20$	0.2945	219	0.3201	195

Table 8. Example 2: L2Err and IterNum vs $\eta = const.$ or r/t with $\tau = 0.01, \Delta t = 10, N_{max} = 1000$.

$$p_0 = \dot{p}_0 = 0.$$

6.3 Comparison with other methods

In this subsection, we compare the behaviors regarding the solution accuracy and the convergence rate between SOAR and three existing methods; that is, the Nesterov's method, the v -method and the dynamical regularization method (DRM) proposed in Zhang *et al.* (2018b). Recall that we use \mathbf{p} as the coefficients of the finite element solution p^h , see **Algorithm 1** for the detail. In all methods, we set $\tau = 0.01$, $\mathbf{p}^0 = \mathbf{0}$, $\mathbf{q}^0 = \mathbf{0}$ if \mathbf{q} is involved, and $\mathbf{p}^1 = \mathbf{p}^0$ if the method is a two-step one. Moreover, in SOAR2 and SOAR4, the total energy discrepancy principle χ_{TE} is used, while, in all other methods, the usual discrepancy function χ is used.

For methods SOAR1-SOAR4, set $\Delta t = 10, \eta = 0.05$ or $5/t$. We remark that on the one hand, these chosen parameters are not the optimal ones; on the other hand, a large range of values of these

parameters could produce satisfactory approximate sources p^h .

For the inverse source problem (1.1) with CCBM formulation, DRM yields the following iteration

$$\begin{cases} \mathbf{q}^{k+1} = \frac{1}{1+\eta\Delta t}\mathbf{q}^k - \frac{\Delta t}{1+\eta\Delta t}(\mathbf{w}_{im}^k + \varepsilon(t_k)\mathbf{p}^k), \\ \mathbf{p}^{k+1} = \mathbf{p}^k + \Delta t\mathbf{q}^{k+1}, \end{cases} \quad k = 0, 1, \dots, \quad (6.2)$$

where $(\mathbf{w}_{re}^k, \mathbf{w}_{im}^k)$ solves (5.9) with \mathbf{u}_{im} replaced by \mathbf{u}_{im}^k , and $(\mathbf{u}_{re}^k, \mathbf{u}_{im}^k)$ solves (5.8) with \mathbf{p} replaced by \mathbf{p}^k . As suggested by numerical experiments of Zhang *et al.* (2018b), we set $\eta = 1, \Delta t = 10$ and the regularization parameter $\varepsilon(t) = 0.1/(t \ln(t))$. It should be mentioned that DRM is not an acceleration method.

For the ν -method, it is defined as ((Engl *et al.*, 1996, § 6.3))

$$\mathbf{p}^{k+1} = \mathbf{p}^k + \mu_k(\mathbf{p}^k - \mathbf{p}^{k-1}) - \omega_k \mathbf{w}_{im}^k, \quad k = 1, 2, \dots \quad (6.3)$$

with $\mu_1 = 0, \omega_1 = (4\nu + 2)/(4\nu + 1)$ and

$$\mu_k = \frac{(k-1)(2k-3)(2k+2\nu-1)}{(k+2\nu-1)(2k+4\nu-1)(2k+2\nu-3)}, \quad \omega_k = 4 \frac{(2k+2\nu-1)(k+\nu-1)}{(k+2\nu-1)(2k+4\nu-1)}.$$

Note that \mathbf{w}_{im}^k in (6.3) has the same meaning as that in (6.2). We select the Chebyshev method as our special ν -method, i.e., $\nu = 1/2$. Moreover, set $\mathbf{p}^1 = \mathbf{p}^0 = 0$ for the implementation of (6.3).

The Nesterov's method is defined by (Neubauer (2017))

$$\begin{cases} \mathbf{z}_k = \mathbf{p}^k + \frac{k-1}{k+\alpha-1}(\mathbf{p}^k - \mathbf{p}^{k-1}), \\ \mathbf{p}^{k+1} = \mathbf{z}_k - \omega \mathbf{w}_{im}^k, \end{cases} \quad k = 1, 2, \dots, \quad (6.4)$$

where $\alpha \geq 3, \mathbf{w}_{im}^k$ has the same definition as that in (6.2) and (6.3). We apply (6.4) to Examples 1 and 2 with parameters $\alpha = 3$ and $\omega = 10$.

δ'	5%		10%		20%	
Example 1						
Methods	L2Err	IterNum	L2Err	IterNum	L2Err	IterNum
DRM	0.0322	369	0.0571	314	0.1260	219
ν	0.0164	53	0.0491	51	0.1183	47
Nesterov	0.0279	42	0.0490	37	0.0969	36
SOAR1	0.0316	14	0.0484	14	0.1214	10
SOAR2	0.0270	17	0.0426	17	0.0909	14
SOAR3	0.0274	19	0.0533	16	0.1079	15
SOAR4	0.0274	19	0.0420	18	0.0958	16
Example 2						
DRM	0.1119	630	0.1089	515	0.1215	372
ν	0.1103	124	0.1036	123	0.1096	122
Nesterov	0.1095	87	0.1114	44	0.1159	42
SOAR1	0.1123	58	0.1095	48	0.1201	36
SOAR2	0.1143	49	0.1109	45	0.1219	35
SOAR3	0.1137	20	0.1105	20	0.1169	18
SOAR4	0.1137	29	0.1152	23	0.1106	20

Table 9. Comparison with the state-of-the-art methods.

The results of the simulations are presented in Table 9, from which we conclude that, with properly chosen parameters, all the mentioned methods are stable and can produce satisfactory solutions. Compared with the dynamical regularization method, all of the other methods offer good results with similar accuracy, but require considerably fewer iterations. Particularly, SOAR1–SOAR4 converge even faster than the well-known Nesterov’s method and the v -method. On the whole, for both Examples, the total energy discrepancy function χ_{TE} leads to more accurate solution than the conventional discrepancy function χ , but with slightly more iterative numbers.

We finally plot the exact and recovered sources with different methods corresponding to $\delta' = 10\%$ in Figure 4 for Example 1. The counterparts for Example 2 are shown in Figure 5. For the conciseness of the paper, we omit the figures corresponding to $\delta' = 5\%$ and 20% .

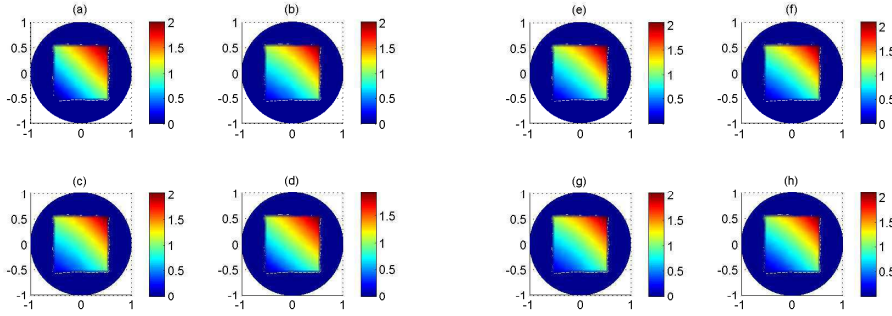


FIG. 4. The true and approximate sources. (a): p^\dagger ; (b): p^h by DRM; (c): p^h by Nesterov’s method (d): p^h by v -method; (e): p^h by SOAR1; (f): p^h by SOAR2; (g): p^h by SOAR3; (h): p^h by SOAR4.

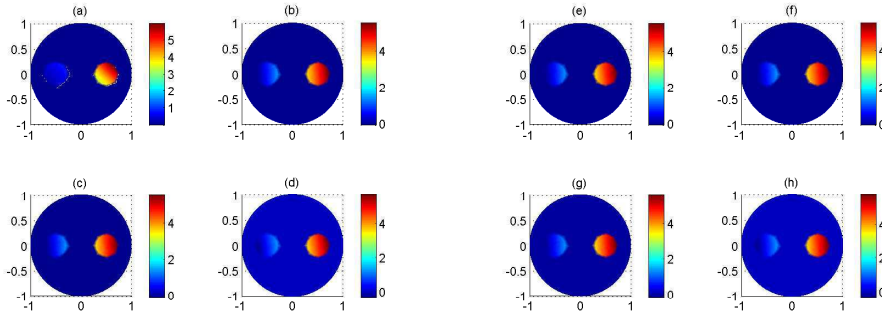


FIG. 5. The true and approximate sources. (a): p^\dagger ; (b): p^h by DRM; (c): p^h by Nesterov’s method (d): p^h by v -method; (e): p^h by SOAR1; (f): p^h by SOAR2; (g): p^h by SOAR3; (h): p^h by SOAR4.

7. Conclusions

This paper is devoted to developing Second Order Asymptotical Regularization (SOAR) methods for solving inverse source problems of elliptic partial differential equations given Dirichlet and Neumann boundary data. We show the convergence results of SOAR for both fixed and dynamic damping parameters. A symplectic scheme is applied for the numerical implementation of SOAR. This scheme yields a novel iterative regularization method. As shown by the numerical results, the proposed SOAR methods are comparable to the Nesterov's acceleration method and the v -method about the convergence rate. Moreover, in this paper, a conventional Morozov's discrepancy principle and a new total energy discrepancy principle are used for the stop criterion. Numerical experiments demonstrate that, in most cases, the newly developed total energy discrepancy principle works slightly better than the conventional Morozov's discrepancy principle. Similar to the Nesterov's acceleration method, the introduced SOAR can also be used to solve to non-linear ill-posed problems in partial differential equations, which will be the one of the topics of our future work.

Acknowledgements

The work of Y. Zhang is supported by the Alexander von Humboldt foundation through a postdoctoral researcher fellowship. The work of R. Gong is supported by the Natural Science Foundation of China (No. 11401304) and the Fundamental Research Funds for the Central Universities (No. NS2018047)

REFERENCES

- AFRAITES, L., DAMBRINE, M. & KATEB, D. (2007) Conformal mappings and shape derivatives for the transmission problem with a single measurement. *Numer. Func. Anal. Opt.*, **28**, 519–551.
- ALVES, C., MARTINS, N. & ROBERTY, N. (2009) Full identification of acoustic sources with multiple frequencies and boundary measurements. *Inverse Probl. Imaging*, **3**, 275–294.
- ATKINSON, K. & HAN, W. (2009) *Theoretical Numerical Analysis: A Functional Analysis Framework (3rd ed.)*. New York: Springer-Verlag.
- ATTOUCH, H., GOUDOU, X. & REDONT, P. (2000) The heavy ball with friction method. i. the continuous dynamical system. *Comm. Contemp. Math.*, **2**, 1–34.
- ATTOUCH, H., CHBANI, Z., PEYPOUQUET, J. & REDONT, P. (2018) Fast convergence of inertial dynamics and algorithms with asymptotic vanishing viscosity. *Mathematical Programming*, **168**, 123–175.
- ATTOUCH, H. & PEYPOUQUET, J. (2016) The rate of convergence of nesterov's accelerated forward-backward method is actually faster than $\mathcal{O}(1/k^2)$. *SIAM Journal on Optimization*, **26**, 1824–1834.
- CHENG, X., GONG, R., HAN, W. & ZHENG, X. (2014) A novel coupled complex boundary method for inverse source problems. *Inverse Problems*, **30**, 055002.
- ENGL, H., HANKE, M. & NEUBAUER, A. (1996) *Regularization of inverse problems*, vol. 375. Springer.
- FERNANDEZ BONDER, J. & ROSSI, J. (2001) Existence results for the p -laplacian with nonlinear boundary conditions. *J. Math. Anal., Appl.*, **263**, 195–223.
- HAIRER, E., WANNER, G. & LUBICH, C. (2006) *Geometric Numerical Integration: Structure-Preserving Algorithms for Ordinary Differential Equations (Second Edition)*. New York: Springer.
- HAN, W., CONG, W. & WANG, G. (2006) Mathematical theory and numerical analysis of bioluminescence tomography. *Inverse Problems*, **22**, 1659–1675.
- HANKE, M., NEUBAUER, A. & SCHERZER, O. (1995) A convergence analysis of the landweber iteration for nonlinear ill-posed problems. *Numerische Mathematik*, **72**, 21–37.
- HUBMER, S. & RAMLAU, R. (2017) Convergence analysis of a two-point gradient method for nonlinear ill-posed problems. *Inverse Problems*, **33**, 095004.

- ISAKOV, V. (1990) *Inverse Source Problems*. New York: American Mathematical Society.
- JOHNSON, C. (2009) *Numerical Solution of Partial Differential Equations by the Finite Element Method*. Mineola: Dover.
- KALTENBACHER, B., NEUBAUER, A. & SCHERZER, O. (2008) *Iterative regularization methods for nonlinear ill-posed problems*. Berlin: Walter de Gruyter GmbH & Co. KG.
- MOTRON, M. (2002) Around the best constants for the sobolev trace map from $w^{1,2}(\omega)$ into $l^1(\partial\omega)$. *Asymptotic Analysis*, **29**, 69–90.
- NEUBAUER, A. (2017) On nesterov acceleration for landweber iteration of linear ill-posed problems. *Journal of Inverse and Ill-Posed Problems*, **25**, 381–390.
- OPIAL, Z. (1967) Weak convergence of the sequence of successive approximations for nonexpansive mappings. *Bull. of the Amer. Math. Soc.*, **73**, 591–597.
- SONG, S. & HUANG, J. (2012) Solving an inverse problem from bioluminescence tomography by minimizing an energy-like functional. *J. Comput. Anal. Appl.*, **14**, 544–558.
- SU, W., BOYD, S. & CANDES, E. (2016) A differential equation for modeling nesterov’s accelerated gradient method: Theory and insights. *Journal of Machine Learning Research*, **17**, 1–43.
- TAUTENHAHN, U. (1994) On the asymptotical regularization of nonlinear ill-posed problems. *Inverse Problems*, **10**, 1405–1418.
- TOLKSDORF, P. (1984) Regularity for a more general class of quasilinear elliptic equations. *J. Differential Equations*, **12**, 126–150.
- VAINIKKO, G. & VERETENNIKOV, A. (1986) *Iteration Procedures in Ill-Posed Problems*. Nauka (In Russian).
- VAZQUEZ, J. (1984) A strong maximum principle for some quasilinear elliptic equations. *Appl. Math. Optim.*, **12**, 191–202.
- ZHANG, Y., GONG, R., GULLIKSSON, M. & CHENG, X. (2018a) A coupled complex boundary expanding compact method for inverse source problems. *J. Inverse Ill-Pose. P.*, DOI, 10.1515/jiip-2017-0002.
- ZHANG, Y., GONG, R., CHENG, X. & GULLIKSSON, M. (2018b) A dynamical regularization algorithm for solving inverse source problems of elliptic partial differential equations. *Inverse Problems*, **34**, 065001.
- ZHANG, Y. & HOFMANN, B. (2018) On the second order asymptotical regularization of linear ill-posed inverse problems. *Appl. Anal.*, DOI, 10.1080/00036811.2018.1517412.

Appendix A. Proof of Theorem 2.3

Denote $q^\delta = \dot{p}^\delta$, $q^\delta(0) = \dot{p}^\delta(x, 0)$, and rewrite (2.6) as

$$\begin{cases} \dot{p}^\delta = q^\delta, \\ \dot{q}^\delta = -\eta q^\delta - w_{im}\chi_{\Omega_0}, \\ p^\delta(0) = p_0, q^\delta(0) = \dot{p}_0. \end{cases} \quad (\text{A.1})$$

By inequality (2.12) in Lemma 2.2, $w_{im}\chi_{\Omega_0}$ is continuously dependent on the source term p , hence, by the Cauchy-Lipschitz theorem, the first order nonautonomous system (A.1) has a unique global solution for the given initial data (p_0, \dot{p}_0) . Furthermore, by the standard arguments in elliptic PDEs theory Cheng *et al.* (2014); Johnson (2009), the global existence of the source function $p^\delta(x, t)$ implies the existence and uniqueness of the elliptic PDEs (2.7) and (2.8), which completes the proof of the global existence and uniqueness of the systems (2.6)-(2.8).

Now, we show the continuity of the solution p^δ with respect to the boundary data.

For any fixed t , define operator $\mathcal{A} : P \rightarrow \mathbf{H}^1(\Omega)$ through $\mathcal{A}p(\cdot, t) = \hat{u}(\cdot, t)$ with $\hat{u}(\cdot, t) \in \mathbf{H}^1(\Omega)$ being the weak solution of

$$\begin{cases} -\Delta \hat{u}(x, t) + \hat{u}(x, t) = p(x, t)\chi_{\Omega_0}, & x \in \Omega, t \in (0, \infty), \\ \frac{\partial \hat{u}(x, t)}{\partial \mathbf{n}} + i\hat{u}(x, t) = 0, & x \in \Gamma, t \in (0, \infty). \end{cases}$$

Denote by $g = g_2 + ig_1$. For any $g \in \mathbf{L}^2(\Gamma)$, define operator $\mathcal{B} : \mathbf{L}^2(\Gamma) \rightarrow \mathbf{H}^1(\Omega)$ through $\mathcal{B}g = \tilde{u}$, where $\tilde{u} \in \mathbf{H}^1(\Omega)$ solves

$$\begin{cases} -\Delta \tilde{u}(x) + \tilde{u}(x) = 0, & x \in \Omega, \\ \frac{\partial \tilde{u}(x)}{\partial \mathbf{n}} + i\tilde{u}(x) = g, & x \in \Gamma. \end{cases}$$

Furthermore, for any $v \in \mathbf{H}^1(\Omega)$, we define $I_m : \mathbf{H}^1(\Omega) \rightarrow H^1(\Omega)$ through $I_mv = v_{im}$. Following standard arguments in the classical PDEs theory, all of \mathcal{A} , \mathcal{B} and I_m are bounded in the corresponding spaces. One the other hand, if we denote $g^\delta = g_2^\delta + ig_1^\delta$, we have

$$w_{im} = I_m w = I_m \mathcal{A} I_m (\mathcal{A} p^\delta + \mathcal{B} g^\delta) =: \mathcal{M} p^\delta + \mathcal{N} g^\delta.$$

Substitute the above equation into (2.6) to obtain

$$\begin{cases} \ddot{p}^\delta(x, t) + \eta \dot{p}^\delta(x, t) + \mathcal{M} p^\delta(x, t) = -\mathcal{N} g^\delta, & x \in \Omega_0, t \in (0, \infty), \\ p^\delta(x, 0) = p_0, \dot{p}^\delta(x, 0) = \dot{p}_0, & x \in \Omega_0. \end{cases}$$

If we define $\delta p = p^\delta - p$, it solves

$$\begin{cases} \ddot{\delta p}(x, t) + \eta \dot{\delta p}(x, t) + \mathcal{M} \delta p(x, t) = -\mathcal{N}(g^\delta - g), & x \in \Omega_0, t \in (0, \infty), \\ \delta p(x, 0) = \dot{\delta p}(x, 0) = 0, & x \in \Omega_0, \end{cases}$$

Applying the Cauchy-Lipschitz theorem again to deduce that for any fixed t , $\delta p(\cdot, t) \rightarrow 0$ in P when $g^\delta \rightarrow g$ in $\mathbf{L}^2(\Gamma)$. Consequently, $p^\delta(\cdot, t) \rightarrow p(\cdot, t)$ in P as $\delta \rightarrow 0$.

Appendix B. Proof of Proposition 4.2

The case with the damping parameter $\eta(t) = r/t$ can be performed along the lines and using the tools of the proof of Lemma 3.4. Hence, it suffices to show the case with the fixed damping parameter $\eta(t) = \eta$.

Denote by $p^\delta(t) = p^\delta(x, t)$, and define the Lyapunov function of the differential equation (2.6) by $\mathcal{E}(t) = V(p^\delta(t)) + \frac{1}{2} \|\dot{p}^\delta(t)\|_P^2$. Similar to the proof of Lemma 3.1, we have

$$\dot{\mathcal{E}}(t) = -\eta \|\dot{p}^\delta(t)\|_P^2. \quad (\text{A.2})$$

Hence, $\mathcal{E}(t)$ is non-increasing, and consequently, $\|\dot{p}^\delta(t)\|_P^2 \leq 2\mathcal{E}(0)$. Therefore, $\dot{p}^\delta(\cdot)$ is uniform bounded. Integrating both sides in (A.2), we obtain

$$\int_0^\infty \|\dot{p}^\delta(t)\|_P^2 dt \leq \mathcal{E}(0)/\eta < \infty,$$

which yields $\dot{p}^\delta(\cdot) \in L^2([0, \infty), P)$.

Now, let us show that for any $p^\dagger \in P$ the following inequality holds.

$$\limsup_{t \rightarrow \infty} V(p^\delta(t)) \leq V(p^\dagger). \quad (\text{A.3})$$

Consider for every $t \in [0, \infty)$ the function $e(t) = e(t; p^\dagger) := \frac{1}{2} \|p^\delta(t) - p^\dagger\|_P^2$. Since $\dot{e}(t) = (p^\delta(t) - p^\dagger, \dot{p}^\delta(t))_P$ and $\ddot{e}(t) = \|\dot{p}^\delta(t)\|_P^2 + (p^\delta(t) - p^\dagger, \ddot{p}^\delta(t))_P$ for every $t \in [0, \infty)$. Taking into account (2.6), we get

$$\ddot{e}(t) + \eta \dot{e}(t) + (p^\delta(t) - p^\dagger, u_{im}(p^\delta(t)))_P = \|\dot{p}^\delta(t)\|_P^2. \quad (\text{A.4})$$

On the other hand, by the convexity inequality of the residual norm square functional $V(p^\delta(t))$, we derive

$$V(p^\delta(t)) + (p^\dagger - p^\delta(t), \nabla V(p^\delta(t)))_P \leq V(p^\dagger). \quad (\text{A.5})$$

Combine (A.4) and (A.5) with the definition of $\mathcal{E}(t)$ to obtain

$$\ddot{e}(t) + \eta \dot{e}(t) \leq V(p^\dagger) - \mathcal{E}(t) + \frac{3}{2} \|\dot{p}^\delta(t)\|_P^2.$$

By (A.2), $\mathcal{E}(t)$ is non-increasing, hence, given $t > 0$, for all $\tau \in [0, t]$ we have

$$\ddot{e}(\tau) + \eta \dot{e}(\tau) \leq V(p^\dagger) - \mathcal{E}(t) + \frac{3}{2} \|\dot{p}^\delta(\tau)\|_P^2.$$

By multiplying this inequality with $e^{\eta\tau}$ and then integrating from 0 to θ , we obtain

$$\dot{e}(\theta) \leq e^{-\eta\theta} \dot{e}(0) + \frac{1 - e^{-\eta\theta}}{\eta} (V(p^\dagger) - \mathcal{E}(t)) + \frac{3}{2} \int_0^\theta e^{-\eta(\theta-\tau)} \|\dot{p}^\delta(\tau)\|_P^2 d\tau.$$

Integrate the above inequality once more from 0 to t together with the fact that $\mathcal{E}(t)$ decreases, to obtain

$$e(t) \leq e(0) + \frac{1 - e^{-\eta t}}{\eta} \dot{e}(0) + \frac{\eta t - 1 + e^{-\eta t}}{\eta^2} (V(p^\dagger) - \mathcal{E}(t)) + h(t), \quad (\text{A.6})$$

where $h(t) := \frac{3}{2} \int_0^t \int_0^\theta e^{-\eta(\theta-\tau)} \|\dot{p}^\delta(\tau)\|_P^2 d\tau d\theta$.

Since $e(t) \geq 0$ and $\mathcal{E}(t) \geq V(p^\delta(t))$, it follows from (A.6) that

$$\frac{\eta t - 1 + e^{-\eta t}}{\eta^2} V(p^\delta(t)) \leq e(0) + \frac{1 - e^{-\eta t}}{\eta} \dot{e}(0) + \frac{\eta t - 1 + e^{-\eta t}}{\eta^2} V(p^\dagger) + h(t).$$

Dividing the above inequality by $\frac{\eta t - 1 + e^{-\eta t}}{\eta^2}$ and letting $t \rightarrow \infty$, we deduce that

$$\limsup_{t \rightarrow \infty} V(p^\delta(t)) \leq V(p^\dagger) + \limsup_{t \rightarrow \infty} \frac{\eta}{t} h(t).$$

Hence, for proving (A.3), it suffices to show that $h(\cdot) \in L^\infty([0, \infty), \mathcal{X})$. It is obviously held by noting the following inequalities

$$0 \leq h(t) = \frac{3}{2\eta} \int_0^t (1 - e^{-\eta(t-\tau)}) \|\dot{p}^\delta(\tau)\|_P^2 d\tau \leq \frac{3}{2\eta} \int_0^\infty \|\dot{p}^\delta(\tau)\|_P^2 d\tau < \infty.$$

From the inequality $V(p^\delta(t)) \geq \inf_{p^\dagger \in P} V(p^\dagger)$, we conclude together with (A.3) that

$$\lim_{t \rightarrow \infty} V(p^\delta(t)) = \inf_{p^\dagger \in P} V(p^\dagger). \quad (\text{A.7})$$

Consequently, we have

$$\lim_{t \rightarrow \infty} V(p^\delta(t)) \leq V(p^\dagger) \leq C_0^2 \delta^2.$$